

BLOOD PRESSURE TREND ESTIMATION FROM ECG AND MULTIPLE PPG
DATA

A THESIS SUBMITTED TO
THE GRADUATE SCHOOL OF NATURAL AND APPLIED SCIENCES
OF
MIDDLE EAST TECHNICAL UNIVERSITY

BY

ATIF EMRE OFLUOĞLU

IN PARTIAL FULFILLMENT OF THE REQUIREMENTS
FOR
THE DEGREE OF MASTER OF SCIENCE
IN
ELECTRICAL AND ELECTRONICS ENGINEERING

DECEMBER 2019

Approval of the thesis:

**BLOOD PRESSURE TREND ESTIMATION FROM ECG AND MULTIPLE
PPG DATA**

submitted by **ATIF EMRE OFLUOĞLU** in partial fulfillment of the requirements
for the degree of **Master of Science in Electrical and Electronics Engineering**
Department, Middle East Technical University by,

Prof. Dr. Halil Kalıpçılar
Dean, Graduate School of **Natural and Applied Sciences**

Prof. Dr. İlkey Ulusoy
Head of Department, **Electrical and Electronics Eng.**

Prof. Dr. İlkey Ulusoy
Supervisor, **Electrical and Electronics Eng., METU**

Examining Committee Members:

Prof. Dr. Nevzat Güneri Gençer
Electrical and Electronics Eng, METU

Prof. Dr. İlkey Ulusoy
Electrical and Electronics Eng., METU

Prof. Dr. Ece Güran Schmidt
Electrical and Electronics Eng, METU

Assoc. Prof. Dr. Cüneyt F. Bazlamaçcı
Electrical and Electronics Eng, METU

Prof. Dr. Canan Kalaycıoğlu
Faculty of Medicine, Ankara University

Date: 09.12.2019

I hereby declare that all information in this document has been obtained and presented in accordance with academic rules and ethical conduct. I also declare that, as required by these rules and conduct, I have fully cited and referenced all material and results that are not original to this work.

Name, Surname: Atıf Emre Oflođu

Signature:

ABSTRACT

BLOOD PRESSURE TREND ESTIMATION FROM ECG AND MULTIPLE PPG DATA

Ofluoğlu, Atıf Emre
Master of Science, Electrical and Electronics Engineering
Supervisor: Prof. Dr. İlkey Ulusoy

December 2019, 76 pages

Blood pressure (BP) measurement using Pulse Transient Time (PTT) is noninvasive cuff-less measurement technique. In this technique, blood pressure pulse is measured from at least two sites of the body. The difference between arrival time of the blood pressure wave to these locations is measured. In this thesis, cuff-less noninvasive blood pressure estimation technique based on PTT measurement is investigated to estimate blood pressure trending. For this purpose, a data collection setup is built. The setup consists of high speed RGB camera and ECG&PPG IC sensor. The camera is used for extracting video PPG (vPPG) signal from the subject's forehead. The IC sensor is used to acquire fingertip PPG and 1 Lead ECG. The experimental data is acquired from 10 volunteers (6 male and 4 female), aged from 21 to 30. For each subject, many data recording sessions are held. Two of the sessions are in rest position and the other two are after exercise to differentiate blood pressure levels among sessions. PTT of each subject for every session is extracted by further processing of the recordings at these sessions. Relation between PTT values and measured blood pressure values by using a gold standard blood pressure measurement device with cuff are investigated using linear regression. Inverse relation is found between PTT and BP. In conclusion, it is showed that blood pressure trending can be estimated by using PTT.

Keywords: Ecg, Ppg, Blood Pressure, Pulse Transient Time

ÖZ

EKG VE ÇOKLU PPG VERİLERİNDEN KAN BASINCI TRENDİ TAHMİNİ

Ofluoğlu, Atıf Emre
Yüksek Lisans, Elektrik ve Elektronik Mühendisliği
Tez Danışmanı: Prof. Dr. İlkey Ulusoy

Aralık 2019, 76 sayfa

PTT ölçümü kullanılarak kan basıncı tahmin edilmesi girişimsel olmayan ve manşetsiz bir ölçüm tekniğidir. Bu teknik kullanılırken, kan basıncı nabızı vücudun en az iki farklı noktasından ölçülmelidir. Nabzın vücudun bu noktalarına ulaşma zaman farkları hesaplanmalıdır. Bu tezde, PTT ölçümleri kullanılarak girişimsel olmayan ve manşetsiz kan basıncı değişimi tahmini irdelenmiştir. Bu amaca uygun olacak şekilde özel bir veri toplama sistemi tasarlanmış ve deneysel ölçümler alınmıştır. Bu sistem, bir yüksek hızlı çekim yapan kamera ve EKG&PPG ölçümü yapabilen bir entegre devre elemanından oluşmaktadır. Entegre devre elamanı, işaret parmağından PPG ve 1 derivasyonlu EKG ölçümü için kullanılmıştır. Yüksek hızlı kamera ise yüzden Video PPG (vPPG) dalgası çıkarmak için kullanılmıştır. Yaşları 21 ile 30 arasında değişen 6'si erkek ve 4'si kadın olmak üzere 10 gönüllünün katılımıyla deneysel ölçümler alınmıştır. Her gönüllü için ayrı birçok veri toplama seansı düzenlenmiştir. Bu seanslardan ikisi gönüllüler dinlenme pozisyonundayken, diğer ikisi ise gönüllüler fiziksel aktivite yaptıktan hemen sonra düzenlenmiştir. Gönüllülere fiziksel aktivite yaptırılarak, seanslar arası kan basıncı değerlerinin değiştirilmesi hedeflenmiştir. PTT ve kan basıncı arasındaki doğrusal ilişki irdelenmiştir. Son olarak, bu tez çalışmasında PTT ölçümü yapılarak ve kan basıncı değişimi tahmini yapılabileceği gösterilmiştir.

Anahtar Kelimeler: Ekg, Ppg, Kan Basıncı, Atım Geçiş Süresi

To my family

ACKNOWLEDGEMENTS

It is my pleasure to get this opportunity to thank everyone who made this thesis possible. First of all, I would like to express my sincere thanks and respect to Prof. Dr. İlkey Ulusoy for her invaluable support and guidance during this long journey. She is one of the best professor I have ever known through my academic carrier. If I weren't settled down to Istanbul, I would definitely continue my academic career by working with her.

I would like to thank everyone who attended to data collection sessions voluntarily. It was a tough process and boring process for anyone of them. I am indebted especially to Farabi Tarhan, Bilgesu Erdoğan, Nurettin Bölücü and Metin Dünder Özkan for their willingness to participate in data collection sessions even if it takes several hours of their priceless time. It wasn't possible to complete the thesis without their precious help. My sincere thanks goes to members of Maxim Integrated Turkey software design center team for their continuous support starting from the idea phase to the end. There are no proper words to describe how supportive and helpful they are. They contributed many ideas to solve challenging problems that I faced through the study. They also attended to data collection sessions as subjects. A special gratitude goes to Yağmur Gök and Alperen Güçlü due to their hands on help and guidance for system design and debug process of the hardware. They didn't even hesitate to help regardless of their workload even though they needed to work overtime just for helping me. There are two best friends of mine I couldn't remunerate their efforts, who are Metin Dünder Özkan and Nurettin Bölücü. They worked way more harder than normal to meet deadline of the projects by taking over my tasks when I am away from the office to deal with the thesis. I also would like to thank Erham Mergen for his support on software design.

I am deeply grateful to my close friends Orkun Tomruk, Özer Gökçe and Önder Tetik for their invaluable support regardless of the problem.

Last but not least; I am both proud and glad for having a family supported me at every aspect of my life unconditionally. I would not have been where I am now without their precious and invaluable help.

TABLE OF CONTENTS

ABSTRACT	v
ÖZ	vii
ACKNOWLEDGEMENTS.....	x
TABLE OF CONTENTS	xii
LIST OF TABLES.....	xv
LIST OF FIGURES	xvi
LIST OF ABBREVIATIONS	xviii
LIST OF SYMBOLS.....	xix
CHAPTERS	1
1. INTRODUCTION.....	1
1.1. Problem Definition.....	1
1.2. Literature Review.....	2
1.2.1. Blood Pressure Measurement Techniques	2
1.3. Pulse Transient Time Method for Blood Pressure Measurement	5
1.4. Blood Pressure Pulse Wave Extraction from Video Recordings (vPPG).....	6
1.5. Remote Blood Pressure Assessment using Video Camera	9
1.6. Purpose of the Study	10
1.7. Thesis Outline	14
2. Theoretical Background	17
2.1. Cardiac Physiology	17
2.1.1. Electrical Activity of the Heart	18
2.1.2. Electrocardiogram (ECG).....	19

2.1.3. Photoplethysmography Measurement (PPG).....	21
2.2. Pulse Transient Time	23
3. Data Collection Setup	25
3.1. Overview of the Data Acquisition Setup.....	25
3.2. Experimental Data Acquisition Procedure	26
3.3. MAX86150 PPG&ECG Integrated Circuit Sensor	28
3.4. MAX86150 (PPG&ECG) Integrated Circuit Sensor Evaluation Kit.....	28
3.5. MAX86150 Sensor Evaluation Kit Software	30
3.6. High Speed RGB Video Camera	32
3.7. IC Sensor Data and Video Camera Data Synchronization.....	34
3.7.1. Sync Using a LED Placed within the Recording Frame.....	34
4. DATA PROCESSING	37
4.1. Handling Output of High-Speed Camera	38
4.2. Detecting Face Landmarks	39
4.2.1. Applying Moving Average Filter to Face Landmarks.....	40
4.3. Cropping a Rectangle Frame from the Subject's Face.....	41
4.4. Averaging the Cropped Rectangle and Bandpass Filter.....	43
4.5. Applying Principal Component Analysis.....	44
4.6. Calculating Time Difference Between Video and IC sensor Recordings	45
4.7. Removing Baseline from the Recorded Signals.....	47
4.8. Pearson Correlation Coefficient (r)	48
4.9. Spearman's Rank Correlation Coefficient (r_s)	50
5. RESULTS	53
5.1. Subject Characteristics	53

5.2. Blood Pressure Measurements of the Subjects	53
5.3. Pulse Transient Time Varieties	54
5.4. Blood Pressure and Pulse Transient Time Correlation	58
6. CONCLUSION	65
6.1. Discussion	65
6.2. Conclusion	66
6.3. Future Work	68
REFERENCES	69
APPENDICES	75
A. Consent Form	75

LIST OF TABLES

TABLES

Table 1: Characteristics of Subjects	53
Table 2: Blood Pressure and PTT measurements for each subject, session.....	56
Table 3: Systolic Blood Pressure vs PTT Pearson Correlation Coefficients	58
Table 4: Diastolic Blood Pressure vs PTT Pearson Correlation Coefficients.....	59
Table 5: Mean Blood Pressure vs PTT Pearson Correlation Coefficient.....	59
Table 6: Additional Blood Pressure and PTT measurements for subject 4 and 10....	60
Table 7: Systolic Blood Pressure vs PTT Pearson Correlation Coefficients	61
Table 8: Diastolic Blood Pressure vs PTT Pearson Correlation Coefficients.....	62
Table 9: Mean Blood Pressure vs PTT Pearson Correlation Coefficients	62

LIST OF FIGURES

FIGURES

Figure 1.1: Invasive arterial blood pressure monitoring system [3, Fig 8.4].....	2
Figure 1.2: Illustration shows PPG sensor located at the back of the Samsung Smartphone [21, Figure 1]	11
Figure 1.3: Apple FaceID System [27].....	12
Figure 1.4: Conceptual Smartphone Design to Enable Mobile Blood Pressure Trending.....	13
Figure 2.1: Cardiac Physiology Diagram	17
Figure 2.2: Cardiac Physiology [24, Figure 11.5]	18
Figure 2.3: Dipole Moment and Corresponding ECG waveform [24, Fig 13.10]	19
Figure 2.4: Single Lead (Lead I) ECG measurement waveform, P, Q, R, S and T waves represents atrial depolarization, depolarization of the interventricular septum, depolarization of the main mass of the ventricles, final depolarization of the ventricle and, ventricular repolarization respectively.[30].	20
Figure 2.5: PPG operation illustration (left one is transmissive and right one is reflective mode).....	21
Figure 2.6: Typical PPG waveform.....	22
Figure 2.7: PTT Demonstration.....	23
Figure 3.1: Data Acquisition Schematic.....	26
Figure 3.2: Data Recording Session timeline	26
Figure 3.3: MAX86150 ECG&PPG Sensor Block Diagram [33].....	28
Figure 3.4: Typical finger placement for ECG&PPG measurement on MAX86150 Evaluation Kit [34]	29
Figure 3.5 ECG Pad Placements: Red, Blue and Black corresponds to Left Arm, Right Arm and Analog ground respectively.....	30
Figure 3.6: MAX86150 Evaluation Kit Software Screenshot.....	31

Figure 3.7: Basler Ace 720-540uc Video Camera	33
Figure 3.8: Produced PWM waveform	35
Figure 3.9: LED Placement.....	35
Figure 4.1: Data Processing Scheme.....	37
Figure 4.2: Detected Facial Landmarks	40
Figure 4.3: Y-Coordinate of one of Facial Landmark.....	41
Figure 4.4: Y-Coordinate of one of Facial Landmark after moving average filter applied	41
Figure 4.5: Cropped Rectangles	42
Figure 4.6: Raw signal of RGB channels of Average of Cropped Rectangle.....	43
Figure 4.7: Bandpass Filtered Signals.....	44
Figure 4.8: Video PPG waveform.....	45
Figure 4.9: Red Channel Signal of Cropped LED Area.....	46
Figure 4.10: Derivative of LED Signal	46
Figure 4.11: PPG waveform before and after Baseline removed.....	47
Figure 4.12: Baseline Removed ECG	48
Figure 4.13: Positive Strong Correlation	49
Figure 4.14: Positive Perfect Correlation.....	49
Figure 4.15: Negative Strong Correlation.....	50
Figure 5.1: PTT calculation.....	55
Figure 5.2: Experimental Data Points of Subject 4 and 10 for 20 session.....	63
Figure 5.3: Experimental Data Points of Subject 4 and 10 for 20 session.....	63

LIST OF ABBREVIATIONS

ABBREVIATIONS

BP – Blood Pressure

SBP – Systolic Blood Pressure

DBP – Diastolic Blood Pressure

MAP – Mean Arterial Pressure

BPMD – Blood Pressure Measurement Device

PPG – Photoplethysmography

rPPG – Remote Photoplethysmography

vPPG – Video Photoplethysmography

ECG – Electrocardiogram

PTT – Pulse Transient Time

rPTT – Remote Pulse Transient Time

BPPW – Blood Pressure Pulse Wave

BPPWV – Blood Pressure Pulse Wave Velocity

PWM – Pulse Width Modulation

LED – Light Emitting Diode

PD – Photo Diode

SpO₂ – Saturation of Peripheral Oxygen

TIFF – Tagged Image File Format

PNG – Portable Network Graphics

LIST OF SYMBOLS

SYMBOLS

r – Pearson's Correlation Coefficient

r_s – Spearman's Correlation Coefficient

CHAPTER 1

INTRODUCTION

1.1. Problem Definition

Blood Pressure (BP) is one of the most vital signs of well-being and health issues. It is also highly correlated with cardiovascular illnesses. High blood pressure causes approximately 54% of strokes and 47% of coronary heart diseases worldwide [1]. An increasing or decreasing trend of blood pressure could cause severe injuries in both the short and long term. Addressing high blood pressure when it is present could prevent most of these diseases. BP of the body is not a stable thing and can be affected by both physiological and environmental changes. It also varies quickly over time without creating easily detectable symptoms. Therefore, over many years, blood pressure monitoring techniques are being developed, and scientists put lots of effort into improving these techniques. Based on these techniques, operator dependent and automatic blood pressure monitoring devices introduced to the market. Most of the automated noninvasive blood pressure monitoring devices are using an oscillometric blood pressure measurement technique. The automatic measurement of blood pressure using that technique requires arm or wrist cuff, a mercury manometer, and a motor to inflate the cuff. With the help of advanced technology, today the size of monitoring devices can be small enough to use in the home. However, still, they are not small enough to carry on within our pockets. To further decrease the size of the monitoring devices requires cuff-less designs. If there were a method where the cuff is removed, and only small sensors are used, blood pressure monitoring would be possible with smartphones or smartwatches. If these smart devices can be used as blood pressure monitoring devices, millions of people can be prevented to have serious injuries by warning them about instant blood pressure changes.

1.2. Literature Review

The literature has been reviewed to find out current blood pressure monitoring techniques, proposed solutions for their drawbacks. In addition to that, cardiac pulse extraction techniques from the video recordings are investigated. Finally, remote cardiac pulse extraction techniques, pulse transient time measurement using these techniques are examined..

1.2.1. Blood Pressure Measurement Techniques

Blood pressure measurement techniques and methods can be separated into invasive and noninvasive.

Intensive care units commonly use invasive blood pressure measurement. The method requires a cannula needle inserted into the artery [2]. Pressure sensors are attached to the cannula to detect pressure on the tip of the cannula. The method has many advantages. The method allows blood pressure monitoring continuously with the best accuracy. It is also possible to measure blood pressure when there is no heart pulse, such as during heart transplant surgery. On the other hand, it has some disadvantages which make it impractical to use in homes. A trained technician should insert the cannula into an artery. It is costly and has many complications over the noninvasive techniques. Consequently, the measurement should be performed in the hospital with trained technicians to ensure patients' safety. The overall schematic of the invasive system can be seen at Figure 1.1.

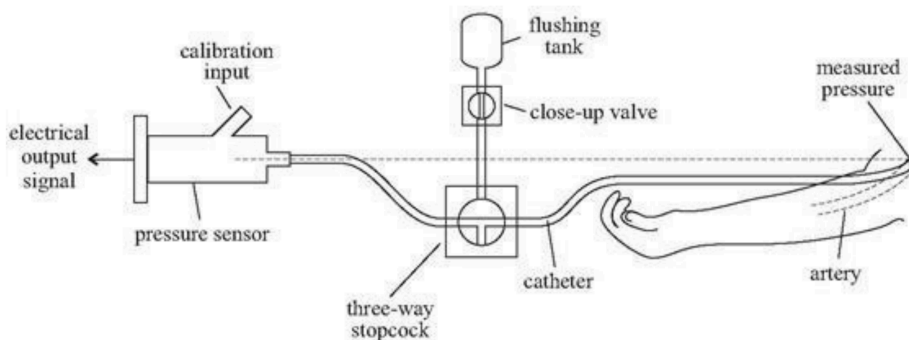


Figure 1.1: Invasive arterial blood pressure monitoring system [3, Fig 8.4]

There are various noninvasive blood pressure monitoring techniques. Most common ones can be listed as auscultatory method, oscillometric method and volume clamp method [2].

In 1905, the auscultatory method was presented in his thesis by Nikolai Korotkoff [4]. The method needs four main components as a cuff, a pressure pump connected to the cuff, a pressure monitor connected to the pump, and a stethoscope. The method has steps as follows. First, a cuff will be placed on the subject's right arm. A stethoscope's diaphragm is placed in the space between the arm surface and the cuff. The stethoscope is listened by operator. The cuff inflated via pressure pump to a higher level of systolic blood pressure to cut blood flow through the artery. Then, the pressure of the cuff will be decreased slowly. At a specific point, the listener starts to hear sounds with a frequency of the heartbeat. That point is marked as systolic blood pressure by reading pressure value on the pressure monitor. Then, the pressure is lowered further until the sounds disappear. The point where the sound disappears indicates the diastolic pressure. The method is widely used in both homes and hospitals due to its ease of use and accuracy. However, there are disadvantages of the system. It is difficult to measure blood pressure without the need for anyone listening to a stethoscope. The one who measures should be trained about the procedure and be familiar with Korotkoff sounds. Due to the need for heavy materials such as cuff, stethoscope, and trained operator, the method isn't suitable for mobile usage.

In 1876, Marey was introduced the oscillometric method to measure blood pressure [4]. It has been discovered before auscultatory, but it wasn't popular until automatic blood pressure monitor devices have become popular. The method also includes an occluding cuff and pressure monitor sensor similar to the auscultatory method. The basic principles of the method can be explained as follows. Like the auscultatory method, the cuff is placed on the right arm of the subject, and then the cuff is started to inflate until the pressure within the cuff reaches systolic blood pressure and consecutively cuts the blood flow through the artery. Then, the pressure in the cuff is

released slowly. At a specific point where pressure oscillations are started to be observed on the pressure monitor of the cuff is marked as systolic blood pressure. As the pressure is released, the oscillations continue to increase until a specific point, and then it decreases. That point is also marked as diastolic blood pressure. That method is widely used by electronic blood pressure monitor devices. There was a long debate about the accuracy of these electronic measurement devices which are using the oscillometric method over the years. Today, it is proven that most of these devices satisfy medical-grade blood pressure measurement having an error of less than ± 5 mm Hg [5]. The method has advantages over the auscultatory method because it can be automated and doesn't need an operator. However, due to the need for the cuff, which makes the devices bulky, it is not feasible for mobile applications.

Another BP measurement method is finger clamp method. It was invented in 1973 by Penaz [4]. The method consists of a cuff, photoplethysmography sensor, and pressure control unit. In this method, unlike the other methods, the cuff is attached to one or more fingers. In 1987, Boehmer improved the technique by introducing a prototype. The prototype is known as FinapresTM. The improved method is named as vascular unloading. In this method, the pressure in the cuff equalized to the blood pressure in the artery, and it was controlled by an electronic control unit. All the time, the pressure is adjusted to be equal to arterial blood pressure. Therefore, the cuff pressure pulsates as the heart beats. Then, utilizing photoplethysmography sensor volume alterations of the artery is measured continuously. Analyzing pressure and photoplethysmography measurements, the system measures blood pressure [3]. This technique is validated by Silke et al. in 1998 [5], and it is now widely accepted for medical use. The most significant advantage of the system is its ability to measure blood pressure continuously and noninvasively. Thanks to its continuous operation, monitoring blood pressure while patients are sleeping is possible. It is crucial for some patients, especially for the ones who need continuous BP monitoring to get proper treatment. However, it requires a cuff which is attached to the fingers. It may be suitable to use

only for a couple of days, but it doesn't have enough comfort to be ideal for mobile applications nor everyday usage.

1.3. Pulse Transient Time Method for Blood Pressure Measurement

Pulse transient time (PTT) can be defined as a time delay between blood pressure pulse arrives two arterial sites. It can also be determined as the inverse of pulse wave velocity. Blood pressure measurement using pulse transient time measurement is proposed by Geddes et al. in 1981 [6]. In their technique, blood pressure pulses are measured from different locations of the arterial vessel using cuff. The pressure of the cuff is released to a point where pulses are detectable. That point is set as systolic pressure. Then, the pressure is released slowly, and pulse delays are observed. Pulse delays shorten as the pressure of the cuff decreases. The point where the pulse delays stabilize is set as diastolic pressure. They used the technique to measure blood pressure of anaesthetized dogs continuously. In 1998, it was showed that there is a strong correlation between pulse wave velocity and blood pressure, age, gender, height by Okada [7].

Over the decades, researchers have lots of interest in cuff-less and noninvasive blood pressure measurement. In 1996, Franchi et al. recorded an ECG and ear photoplethysmography waveform of the subject together to measure PTT. While recordings are taken place, intra-aortic blood pressure is also monitored simultaneously. They have found that PTT and blood pressure are negatively correlated. Systolic blood pressure and PTT Pearson linear correlation coefficient (r) are equal to -0.64 [8]. After these studies' promising results, researchers studied many times with different methods to measure PTT and correlate with blood pressure. In 2015, Patzak et al. measured PTT by using ECG and finger PPG sensor. They also recorded intra-arterial blood pressure by using invasive catheter blood pressure measurement method. In their study, 12 healthy subjects are involved, and their ages were changing from 21 to 53 years old. They used the Pearson coefficient and The Bland—Altman plot to evaluate their results. They find out that systolic intra-arterial

blood pressure is highly correlated with blood pressure $r = 0.947$ ($p < 0.01$). The limits of the agreement were $\pm 19\text{mmHg}$ according to The Bland—Altman plot. They stated that the results encourage to study on PTT and BP relation more deeply [9].

1.4. Blood Pressure Pulse Wave Extraction from Video Recordings (vPPG)

Photoplethysmography (PPG) is used for decades to measure blood volume changes and extract blood pressure pulse waves (BPPW) by placing an optical sensor at the skin. The method requires a device that has contact with the finger, ear, toe, etc. It is so simple and cost-effective to use in hospitals. However, sometimes, it is needed to measure PPG remotely where contact to skin is not possible. Detecting BPPW without having a contact sensor to the skin could be named as remote PPG (rPPG). If BPPW could be sensed remotely, there will be a broad range of its applications from healthcare to security. For example, the heart rate of the person can be monitored remotely with rPPG. That will enable heart rate monitoring of premature babies stays in neonatal intensive care units without contact. Athletes' heart rate and SpO2 could be measured while they are doing their sport. There won't be any dangling cables nor any measurement device attached that may affect their performance. If there is surveillance cameras in emergency situations where one or more person injured badly, the cameras could measure injured persons heart rate and reveal their vital signs and medical professionals could come there for emergency help well-prepared.

Due to the usability of rPPG in these situations, rPPG has got lots of attention from researchers. In 1997, Grenaker used radar imaging to measure heartbeat and respiration by extracting PPG remotely. It has been shown that remote blood pressure pulse measurement is possible [10]. In 2007, the blood pressure pulse was measured by Garbey et al. using a thermal camera. They have used the temperature of the skin as a cardiac signal and reached the performance of 88.52% to 90.33% [11]. In 2010, Poh et al. proposed a new technique to extract cardiac pulses from video recordings. They showed that cardiac pulses could be extracted from a simple RGB webcam. The technique allows measuring heart rate, SpO2 contactless, and remotely. It makes heart

rate measurement possible for almost every electronic device that has a simple RGB camera [12]. These can be listed as personal computers, smartphones, and tablets. If rPPG measurements have good enough accuracy, this measurement will be enabled for millions of people who have these electronic devices.

Since then, plenty of studies have been conducted to improve the accuracy of rPPG from the sequence of the RGB images or videos. Most of these used studies used blind source separation techniques (BSS) such as PCA and ICA [12], [13]. In 2013, de Hann et al. proposed a chrominance-based method to measure rPPG and extract heart rate for the subjects are in rest and exercise state. Their technique outperformed BSS techniques, especially when the measurements are taken place while the subjects are exercising. [14]. In 2016, Iozzia et al. developed a new method for rPPG extraction from video recordings. They used de Haan et al. 's chrominance model [14] and then applied skin tone correction, motion artifact reduction to get better accuracy. While the previous studies focused on heart rate accuracy, they focused on interbeat intervals (IBI). Their method is able to measure IBI with an accuracy of 92%. They also showed that how the region of interest (ROI) of the subject's face affects the accuracy of the IBI measurement. If the nose area is selected as a rectangle ROI, it produces the best results. [15]. Accurately measuring IBI is crucial because it makes remote pulse transient time measurement possible by comparing BPPW arrival times to different sites of the body [16].

Most of the studies in the literature extract rPPG signal by using RGB spectrum cameras. There are lots of environmental noises that decrease the accuracy of rPPG when the camera is operating in the RGB spectrum. They tend to get affected by sunlight illumination changes. They also don't work in dark environments. On the other hand, if infrared (IR) or near-infrared (NIR) cameras are used for rPPG extraction, these issues could be solved. In 2015, van Gastel et al. investigated whether motion robust rPPG is possible or not by using IR cameras. To do so, they set up a synchronized four-camera system to measure BPPW remotely from the subjects' faces. All the four cameras were RGB cameras, but three of them were having visible

light blocking filters on their lenses. The filters only allow three different bands of the IR spectrum. By doing so, they used RGB camera's ability to sense IR. Six participants are involved in this study. Their skin color can be divided into three, according to the Fitzpatrick's scale. They applied current state-of-art methods or RGB color space to extract rPPG waveform from the video recordings. They concluded that using an IR camera for rPPG is feasible and could be applied to different skin tones without losing accuracy. Even though IR cameras performing less accurate than RGB cameras, there is not much difference. While IR cameras have a mean absolute error of 1.53 BPM, RGB cameras have 1.20 BPM for heart rate extraction [17]. In 2016, Lindqvist et al. set up a system to extract heart rate from NIR videos. They have recorded video recordings of subjects' faces with a monochromatic camera having NIR lenses to only allow NIR spectrum to pass through. By doing so, they eliminate RGB spectrum. They also found out that RGB videos are more responsive to blood volume changes at skin arteries than NIR videos. However, they concluded that it is possible to detect BPPW from video recordings as showed before [17]. Their method decreased heart rate measurement mean error to 1.03% [18]. In 2018, Chen et al. investigated remote BPPW and respiration rate measurement with Leap Motion Controller. It is a device which is mainly used to control personal computer. But, it has a simple 62 fps IR camera and lightning LEDs. They recorded NIR videos of 12 participants' neck while recording their ECG. They have measured HR by extracting BPPW from the IR camera with a mean absolute error of 0.54 BPM. They showed that performance of the setup doesn't change as the lightness condition changes. The camera is able to operate in the dark environment by having illuminator LEDs operating in IR spectrum [19].

To sum up, the principle of measurement of BPPW from a video is very similar to the contact photoplethysmography waveform. As blood volume changes in the arteries beneath to skin, light absorption, and reflection coefficient of the skin changes. It results in fluctuations in the pixel values of the sequential frames of the video. If these fluctuations are captured by properly image processing techniques, the BPPW will be

extracted. As detailed in previous paragraphs, the key points are finding the best method to acquire recordings and apply correct techniques to eliminate environmental noises from these recordings. Thanks to today's advanced technology, most of the electronic devices which are used in everyday life have built-in cameras. These cameras make rPPG measurement available to millions of people. There are free apps at the market that can measure HR using rPPG like Cardiio.

1.5. Remote Blood Pressure Assessment using Video Camera

As detailed in the previous sections, it is shown many times that PTT and BP are highly correlated [9]. It is also shown that remote PPG measurements are possible. Its accuracy is getting better and better over the years as the researchers put their interest upon the topic. Merging these two concepts could make remote blood pressure measurement possible. If remote blood pressure measurement is available, it can be adapted to mobile devices and blood pressure related health issues could be avoided by detecting abnormal blood pressure changes in advance only by using mobile devices that we are currently using such as smartphones or smartwatches.

In 2016, Jeong et al. hypothesized that remote blood pressure assessment could be possible by measuring rPPG waveforms from two distant sites of the body. To do so, they prepared a unique setup to measure pulse transient time remotely from the hand and face of the subjects. They utilized a high-speed camera which is capable of recording high frames rate videos. They pointed the camera towards the subjects' faces and asked them to raise their hands and place right next to their head. They proposed a data acquisition procedure with three sessions as rest, exercise-1, and exercise-2. After each session, they recorded 1-minute videos of subjects' face and hand with 420 frames per second. At the same time, they recorded contact PPG and ECG waveforms. Every subject is visited three times. Hence, nine recordings are held for all subjects to variate their blood pressure as much as possible while recordings are taken place. They found that the inter-person average Pearson's correlation coefficient of contact PTT and rPTT is between 0.85 ± 0.08 . They also found that the correlation between rPTT

and systolic blood pressure is 0.632 to 0.960 with $p < 0.05$. Even though, they could not find a method to assess blood pressure directly from PTT yet, these results are too promising for mobile blood pressure trending estimation [20].

In 2017, Zhang et al. investigated contact PTT and rPTT relation deeply. First, they proposed two PPT modalities as Ref-PTT and IC-PTT. Time delay in between signals acquired only from contact PPG sensors at face and fingertip is named as Ref-PTT. Time difference of remote PPG from face video and contact PPG at finger is named as IC-PTT. They have used a simple 25 frame RGB video camera and up sampling for rPPG extraction. Twenty-nine subjects attended to their study. Their data acquisition procedure for each subject includes four stages. For each stage, blood pressure measurements are taken by an electronic sphygmomanometer with cuff having an error of ± 3 mmHg. Before and after each BP measurement, contact PPGs and video of subjects' faces are recorded. Subjects were in the resting position for two of the stages. In the other two stages, subjects were exercising with hand-grip. Therefore, they gathered BP and PTT measurements for four sessions. They have found that contact Ref-PTT and IC-PTT correlated strongly for most of the subjects ($r > 0.6$). They also noted that systolic blood pressure (SBP) is inversely correlated for 75.9% of the subjects [21].

Consequently, all of these studies show that remote blood pressure measurement or trending estimation could be possible by comparing two PTT measurements taken at different time instances with correct calibration.

1.6. Purpose of the Study

The study in this thesis is inspired by technological improvements done by the mobile and semiconductor industry.

First of all, today's smartphones are well equipped with lots of sensors that are also capable of getting biological signals. As an example, UpToDate smartphones are equipped with PPG sensor on the back of its case. By using this sensor, users can measure their heart rate, heart rate variability, and SpO₂. These were brand new

features at times they announced. They have become so popular over the years. Then, now almost all the smartwatches come with PPG sensor installed.

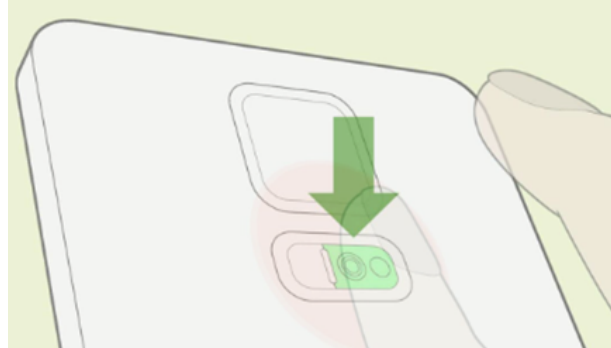


Figure 1.2: Illustration shows PPG sensor located at the back of the Samsung Smartphone [21, *Figure 1*]

There was another breakthrough. It is shown in recent studies that arrhythmia can also be detected by interpreting PPG measurements [23]. Apple has launched “Apple Heart Study” program in November 2017. The study was a collaboration with Stanford Medicine and asking for volunteer users to collect PPG data from their Apple Watch to improve AFib detection algorithm being developed by Apple. After a year later, Apple announced its brand-new smartwatch Apple Watch 4 to the market. Apple Watch Series 4 has one of a kind features like AFib and unusual heart rate detection. In December 2018, Apple made AFib detection and ECG measurement available on its Apple Series 4 watches [24]. It has been reported from many sources that Apple Watch Series 4 has already started to save people's lives only few days after the feature is enabled. [25].

Moreover, in January 2019, a semiconductor company, Maxim Integrated recently announced a brand-new IC product named MAX86150. It is one of a kind biosensor IC that can collect low noise two-channel PPG and single-lead ECG in sync up to 1600Hz with ambient light rejection. It is a medical-grade sensor and one of the best in the market. It is the first IC that collects ECG&PPG in-sync [26]. Thanks to its synchronous data acquisition, it is one of the best candidates for pulse transient time measurements between ECG and PPG waveforms.

In addition to all these advancements, there is one other which is not designed to acquire bio-signal but can be. Apple ships its recent smartphone with FaceID technology. FaceID technology consists of an infrared camera, dot projector, and flood illuminator as shown in Figure 1.3. The system is specially designed to recognize and extract features from the user's face. It operates in the IR spectrum to eliminate noise introduced by optical light spectrum to enhance its face detection ability. Furthermore, it can operate in dark environments without compromising its performance. Due to privacy concerns, Apple doesn't allow anyone to access raw FaceID data.

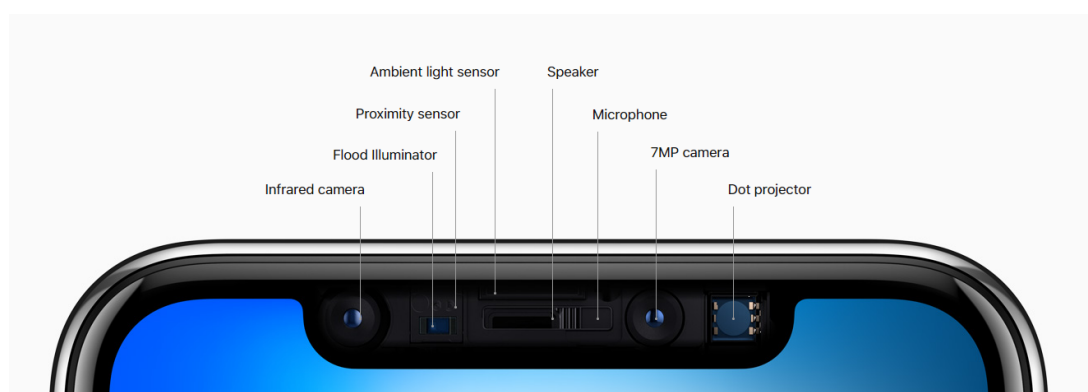


Figure 1.3: Apple FaceID System [27]

In the literature review, it is discussed that there are many studies to measure the pulse transient time of the subjects using video camera projected directly to their face and there are promising results obtained [20], [21]. The studies also suggest that IR spectrum cameras could perform better compare to RGB spectrum cameras when there is not equally distributed lightning or even the environment isn't illuminated [17], [19]. Contrary to RGB cameras, the performance of IR cameras could be enhanced by using a small IR illuminator even when daylight is present. It is not possible for RGB cameras because the sun is far more powerful than any illuminator that has a reasonable size. All of these would make the FaceID system a perfect fit to retrieve the blood pressure pulse wave for mobile applications if raw data was available.

If all these achievements and literature survey findings are considered, it can be thought that blood pressure trending can be estimated using a smartphone. In this

thesis, a conceptual smartphone is designed to be used for blood pressure trending estimation.

The conceptual smartphone should house MAX86150 (ECG&PPG sensor) and a camera system which is fast enough to acquire images with the frequency of PPG&ECG sensor to have better sync and accuracy. PPG sensor should be placed at the back of the smartphone so that user's index finger could reach to the sensor and placed on top of it similar to today's smartphones have PPG sensor already. The camera should be placed right near to selfie camera of the smartphone similar to the FaceID camera. It could capture video recording of the face of the user while the user looks towards to smartphone's screen. Most of today's smartphones have separate metal antennas on the corners of their bodies on the left and right side. These antennas could be connected to MAX86150's ECG inputs separately. That design would allow acquiring two PPG waveforms from the different sites of the body (finger and face) and a single ECG waveform. User should place his/her hands and look at the camera, as shown in *Figure 1.4*. Eventually, these PPG and ECG waveforms made two PTT measurements possible which correlates linearly with blood pressure as shown in the previous studies.

In conclusion, it is hypothesized that a specially designed smartphone user can monitor his/her blood pressure trending anytime and anywhere without carrying heavy, unwieldy blood pressure monitoring devices. There is not any smartphone designed in that way available yet.

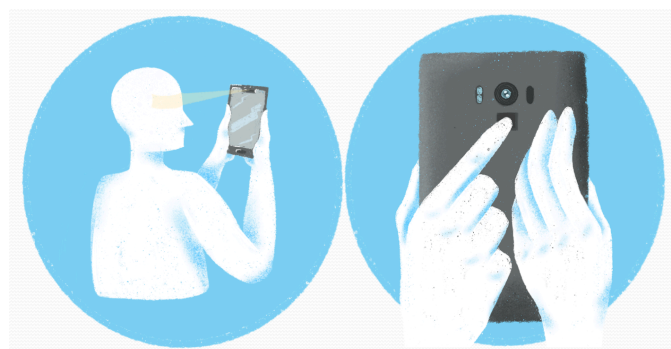


Figure 1.4: Conceptual Smartphone Design to Enable Mobile Blood Pressure Trending

The thesis is mainly focused on two things. First, validation of conceptually designed smartphones' ability to measure PTT by utilizing the PPG&ECG IC sensor and RGB camera. Second, linear relation in between BP and PTT to estimate BP trending using the conceptual smartphone.

To verify the conceptual design and blood pressure trending estimation method, a special kind of data collection system is designed. The system consists of a high-speed camera, ECG&PPG IC sensor, synchronization LED, gold standard automatic blood pressure monitoring device and PCs as recording end. Blood pressure, PPG, ECG and video recordings of the subjects are collected having four different data recording sessions. Ten subjects are attended to this study voluntarily. Their data is processed by having their signed consent. The consent form can be found at Appendix section. Then, their data is processed to extract PTT. Finally, PTT and BP values of each subject are compared by linear regression method.

1.7. Thesis Outline

The thesis started with the literature review and purpose of the study in Chapter 1. In the literature review part, the techniques of blood pressure measurements are examined. Remote blood pressure assessment techniques and their feasibility to be packed into a smartphone are also discussed. Then, in the purpose of the study section, the inspiration of the thesis is explained. Finally, it is hypothesized that blood pressure trending could be estimated by a conceptually designed smartphone that made from the components that are available in today's technology. In the Chapter 2, theoretical background information of cardiac physiology and cardiac-related bio-signals are explained. By doing so, what the grounds of the bio-signals are and how they are related to BP is explained. In chapter 3, a data collection setup and a data acquisition procedure are detailed. These are specially designed and used to verify the hypothesis suggested in Chapter 1. Steps and requirements of the design of the data collection are given in detail. The challenges of the setup are discussed by explaining how they are overcome. In chapter 4, data processing steps are given in detail. Every step is

explained in detail by mentioning why they are needed and what their advantageous over their alternatives are. In chapter 5, the analysis metric for the results (Pearson Correlation Coefficient and Spearman's Correlation Coefficient) are explained. Collected data at the sessions and data processing outputs are given. These are linked to the results of the study. Finally, in Chapter 6, discussion on the results and future work prospects are given by discussing the things that have affected the results, and the things could be done to improve the results.

CHAPTER 2

THEORETICAL BACKGROUND

2.1. Cardiac Physiology

The human heart is a group of muscles that pumps blood into the circulatory system at regular intervals. It has four chambers, namely: left atrium, right atrium, left ventricle, and right ventricle. Systematic movement of the heart muscles is called as Cardiac Cycle. The cycle consists of two main stages as Diastole and Systole. During the diastole stage, the heart muscles relax consecutively chambers start to fill with blood. In contrast with diastole, during the systole stage heart pumps blood to vessels by contracting its muscles. Blood is pumped from the ventricles of the heart to the aorta. Aorta splits the blood into three major arteries; left subclavian artery, left common carotid artery and brachiocephalic trunk. Then, the pumped blood travels along the body. The cardiac cycle continues without interrupting for the whole life span of a person. The rhythm of the cycle is controlled by the nervous system. Due to the cardiac cycle, blood pressure pulse travels along arteries as the heart continues to beat.

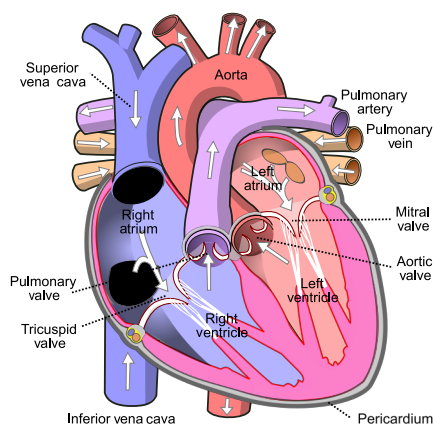


Figure 2.1: Cardiac Physiology Diagram

2.1.1. Electrical Activity of the Heart

A human heart beats approximately 60 times per minute for an adult. There are two mechanisms have control over the heart activity, namely the autonomous nervous system and nodal system. Autonomous nervous system has control over how frequent the heart should beat. It can either increase or decrease the beat to beat intervals depend on the body's mental situation. Nodal system is a closed-loop system that ensures beat continuity even though there aren't any external stimuli present from the autonomous nervous system. It also ensures 75 beat per minute even though there are not external stimuli from the autonomous nervous system to keep the body alive even when brain damage occurs. Nodal system consists of its own pacemaker called Sinoatrial node (SA) and AV node. Each SA node depolarization periodically initiates cardiovascular cycle by contracting atriums and creates an electrical pulse. Approximates 0.1 seconds after, electrical pulse reaches to AV node and travels along with the bundle of his and spreads through the ventricle walls. Then, the ventricles contract. This electrical activity creates a dipole moment which could be sensed by external electrodes noninvasively.

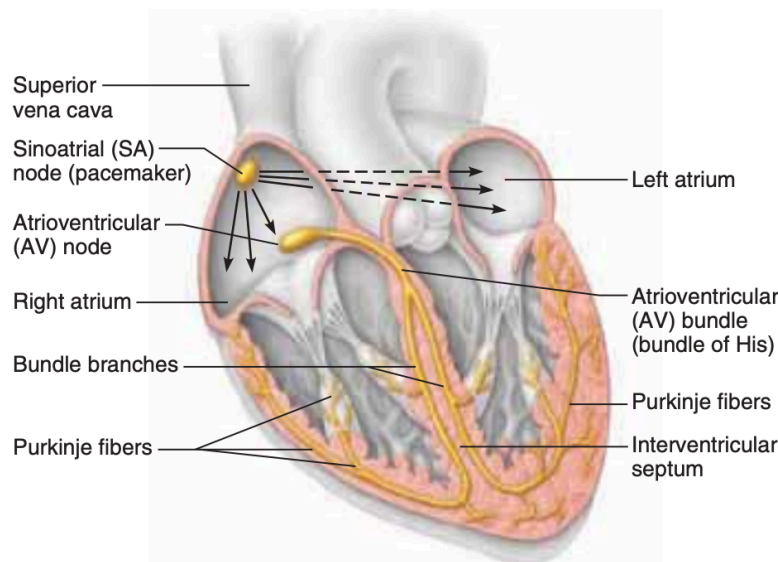


Figure 2.2: Cardiac Physiology [24, Figure 11.5]

2.1.2. Electrocardiogram (ECG)

Electrical activity within the heart creates depolarizations of the cardiac muscles and nerves. These physiological activities create a rotating electrical dipole moment. The dipole moment can be sensed from outside using simple electrodes and proper amplifier circuitry. ECG can be defined as the recording of that electrical activity of the heart. There are different ECG measurement systems. The most common ones are the Single Lead system, Einthoven Triangle, 10 Lead Waller system, and 12 lead system. As the electrode number increases, diagnosis of the accuracy of the ECG measurement and the information it gathers increases. For the cardiac-related illnesses diagnose, 12 lead ECG system is accepted as a medical-grade ECG measurement system. It is mostly used in hospitals for most of cardiac-related diagnostics. In this thesis, the main goal was the measurement of pulse transient time for the mobile application of blood pressure trending. So, it is not needed to use any ECG measurement system which is more complicated than the single-lead ECG system. The single-lead ECG system satisfies the requirements for the study in this thesis. An example waveform of single-lead ECG measurement can be seen in Figure 2.4. ECG measurement is crucial in this thesis because it points to the time instance when the heart pumps the blood to arteries. In addition to that, it reveals the heart rate.

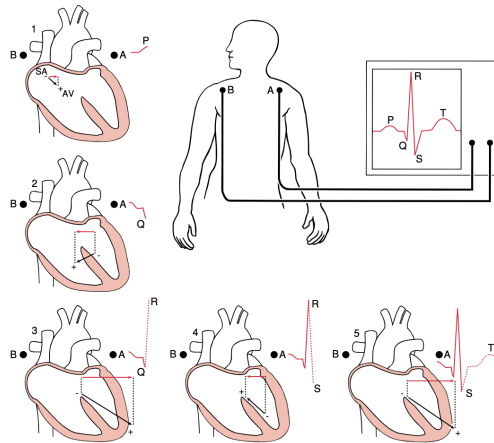


Figure 2.3: Dipole Moment and Corresponding ECG waveform [24, Fig 13.10]

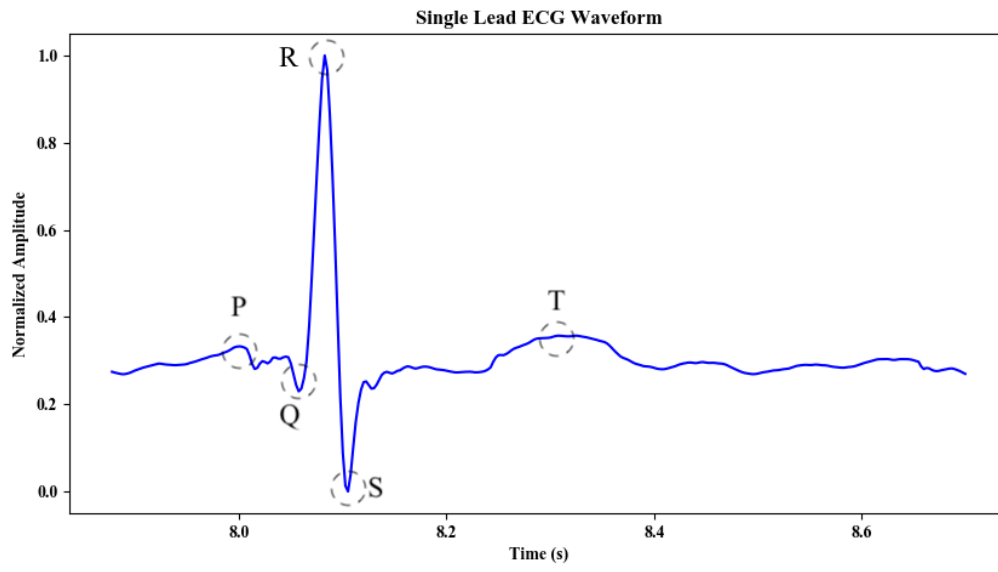


Figure 2.4: Single Lead (Lead I) ECG measurement waveform, *P*, *Q*, *R*, *S* and *T* waves represents atrial depolarization, depolarization of the interventricular septum, depolarization of the main mass of the ventricles, final depolarization of the ventricle and, ventricular repolarization respectively.[30].

2.1.3. Photoplethysmography Measurement (PPG)

Photoplethysmography is a noninvasive plethysmography technique to detect blood flow changes in the peripheral circulation. There are two types of PPG measurement techniques named as transmissive and reflective. Both include at least two main components, which are an light-emitting diode (LED) and a photodiode (PD). Depending on the optical design, the number of LED and PD can increase to get better signal quality. LED generates a light pulse through tissue, and then PD detects transmission or reflection of the light based on whichever mode is used. As blood pressure pulse flows through the arteries, the volume of the arteries changes slightly, and these changes result in reflection or transmission of the LED light change. These variations are detected by a photodiode, and PPG waveform is constructed. The sketches in Figure 9 show the two operation modes of the PPG. While the reflective mode used, Red-colored LED produces light pulses at the bottom side of the fingertip, and PD collects the reflected light by placing just next to the LED. When the transmissive mode is used, the red-colored LED again produces light pulses from the bottom of the fingertip. However, in contrast to reflective mode, PD collects transmitted light on the upper side of the fingertip.

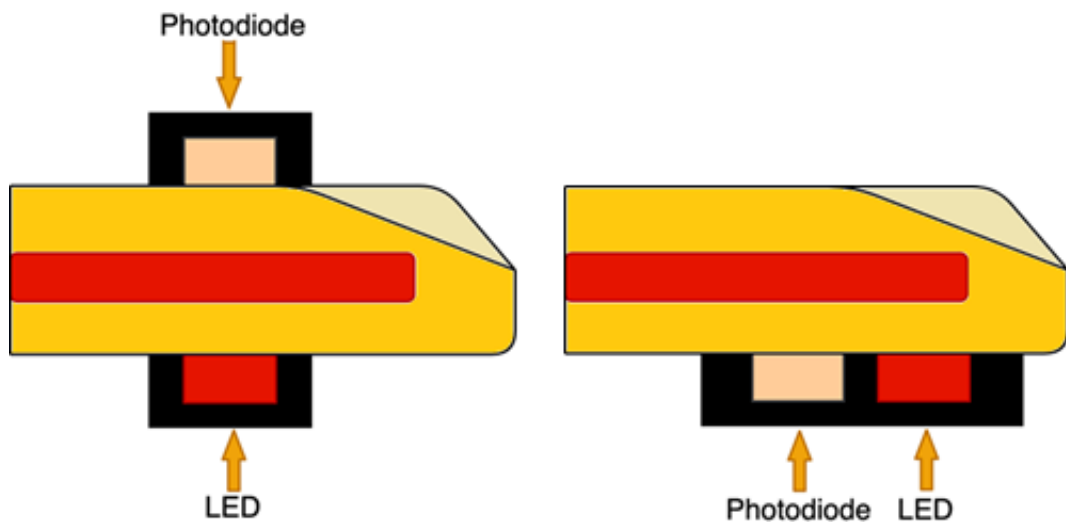


Figure 2.5: PPG operation illustration (left one is transmissive and right one is reflective mode)

Both techniques have advantages and disadvantages; the reflective mode can be applied almost all skin regions to the body. On the contrary transmissive mode could only be applied to thin parts of the body and where there is no bone present such as fingertip and earlobes. The transmissive mode has a better signal to noise ratio than the reflective mode.

It provides lots of vital information regarding the wellness of the cardiovascular system. Commonly used ones are followings; arrhythmia detection, heart rate variability, hemoglobin, SpO2 measurement, and pulse transient time. Thanks to recent technological improvements, photoplethysmography measurement devices are small enough to fit into cellphones and smartwatches. Starting from Samsung Galaxy S5, Samsung Galaxy series phones are equipped with a PPG sensor on their back. When smartwatches hit the market, they are also equipped with the PPG sensor on their back which measures forearm photoplethysmography to detect SpO2 and heart rate. A typical reflective mode PPG is shown in *Figure 2.6*. The waveform of the figure is generated from the experimental data collected for this thesis.

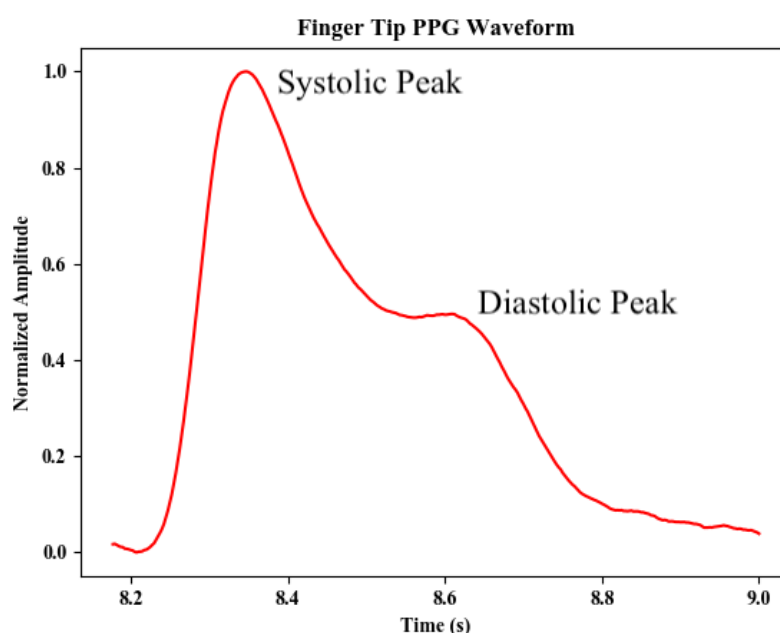


Figure 2.6: Typical PPG waveform

2.2. Pulse Transient Time

Pulse Transit Time (PTT) can be defined as the time difference in between Blood Pressure Pulse Wave (PPPW) to propagate from the heart through a length of the arterial tree to different sites of the body. As blood pressure of the body changes, the elasticity of the arteries changes [31]. Therefore, the flow speed of the blood through arteries changes. It is thought that there is a strong correlation between PTT and Blood Pressure, and many scientists gave their attention to investigate this relation over the years [32]. Figure 2.7 shows three different waveforms obtained at three different sites of the body. The waveforms of the figure are generated from the experimental data collected only for this thesis. ECG R peak indicates the instant when blood starts its flow from the heart chambers to arterial vessels. On the other hand, the PPG waveforms show the instant when the blood pressure wave reaches the body sites where PPG signals acquired. They are fingertip and forehead. Dash lines and marked point on the PPG waveform indicate highest blood pressure wave change in the arteries.

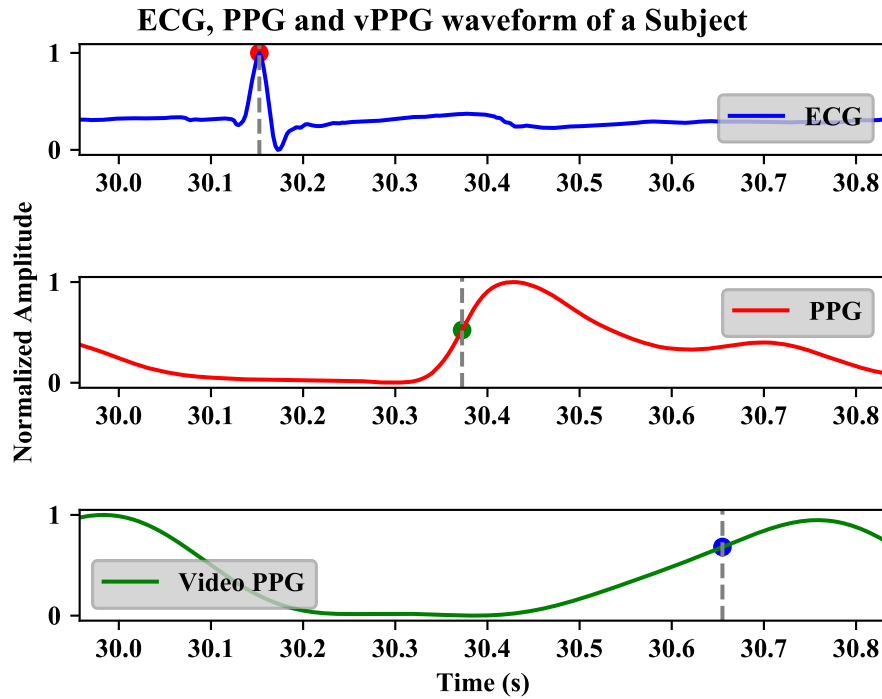


Figure 2.7: PTT Demonstration

CHAPTER 3

DATA COLLECTION SETUP

The conceptually designed smartphone system aims to enable blood pressure trending estimation having two main components; PPG&ECG sensor and a video camera. In order to verify the system, an experimental setup need to be established. The setup should acquire PPG&ECG signals from the IC sensor and video PPG waveform from the video recording device. Then, the signals acquired form these components should be processed to have blood pressure trending estimation based on PTT extraction. To do so, the estimation results should be compared to a gold standard blood pressure measurement to evaluate whether blood pressure trending could be estimated using PTT. Therefore, as an initial step, a data collection setup and procedure are established.

3.1. Overview of the Data Acquisition Setup

Data acquisition system is setup with four main components as follows;

- 1- High Speed RGB camera by Basler (Figure 3.7)
- 2- MAX86150 Evaluation Kit (*Figure 3.5*)
- 3- MAX86150 Evaluation Kit Software (*Figure 3.6*)
- 4- Synchronization LED (Figure 3.9)
- 5- Wireless Blood Pressure Monitor device by Withings.

A high-speed camera (Basler Ace 720-540uc) is placed on a tripod to have a better field of view adjustments while having a stable placement *Figure 3.1*. Then, the tripod is glued on the table to make sure the tripod not shake and displace with small vibrations. A chair is placed in front of the camera so that the subjects can sit and have the least amount of head movements possible. MAX86150 Evaluation kit is ordered through Maxim Integrated's website to get in sync two-channel PPG and Single Lead

ECG waveforms. ECG pads are placed on the inner side of the left and right wrist. Subjects placed their right index finger on top of the PPG sensor. The evaluation kit is connected to a Windows running PC via USB 2.0/3.0. On the other hand, the high-speed camera is connected to a Macbook. PC's are responsible for both configurations of the connected devices and data storage. The high-level scheme of the system can be seen in *Figure 3.1*.

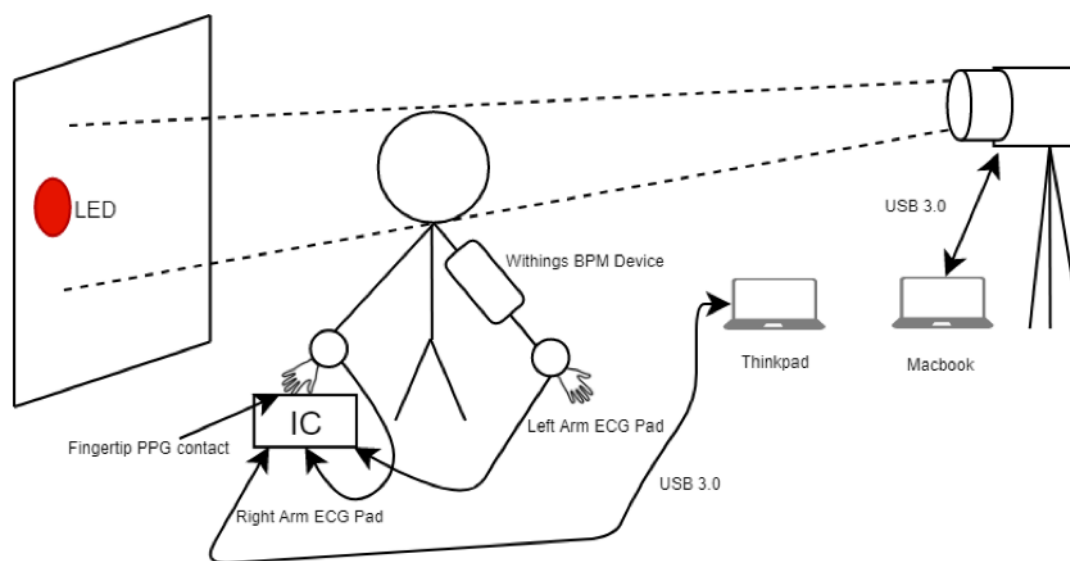


Figure 3.1: Data Acquisition Schematic

3.2. Experimental Data Acquisition Procedure

Blood pressure, video recording, and PPG&ECG measurements are recorded for four different sessions for each subject participating in this study. Subjects were in rest positions for two of the sessions. The other two data collection session is held just after exercises to differentiate the subject's blood pressure between sessions. The timeline for the sessions is seen in Figure 3.2.



Figure 3.2: Data Recording Session timeline

In this figure; Rest blocks represent the duration when subjects are in rest position and sitting on the chair. BPM stands for blood pressure measurement by Withings BP

monitor device. Each BPM block indicates at the time BP measurement is taken. REC blocks represent the time when the recording session is held. At the beginning of each data collection procedure. Each subject sits on the chair for five minutes in the rest position to stabilize their blood pressure. Then, their blood pressure is measured by an automatic blood pressure measurement device by Withings BPMD to acquire gold standard BP values with an error of ± 3 mm Hg. Then, a recording session is started to acquire data while subjects are in the rest position and their blood pressure levels at their minimal. After the recording is completed, subjects are asked for 1-minute exercise to increase their blood pressure level. Right after they exercise, BP is measured by Withings BPMD, and the recording session is held. After the recording is completed. Subjects stayed in the rest position, and their BP is measured with an interval of 5 minutes by Withings BPMD. When BP levels reached near to their first measurement in the rest position, the second rest session is held, and data is recorded. Finally, subjects are asked to exercise 2 minutes to increase blood pressure further compare to the previous exercise section. Right after they exercise, again their BP is measured, and data recording session is held. BP is measured one more time After data acquisition finished to average the last two BP measurements, because it decreases quickly over time for healthy adults. It is better to average the BP measurements taken right after exercise and right after data recording than only having single measurement before each video recording. Exercises are differed from subject to subject. Each subject is asked to which exercise is most suitable for him/her and will change his/her heart rate significantly. By doing so, any possible injuries are avoided. Some of the subjects who are more athletic exercised with push-ups and squat jumps, some who not athletic just exercised by running in place. Running in place stands for imitating run without displacement.

3.3. MAX86150 PPG&ECG Integrated Circuit Sensor

Maxim Integrated Products Inc. recently announced its newest and best in class sensor MAX86150 to the market. MAX86150 can measure single-lead ECG and two-channel (Infrared and Red) PPG in sync. It has high enough accuracy to be a medical-grade sensor and can sample up to 1600 Hz. It synchronizes ECG and PPG waveforms inside of the IC. These features make the IC one of the best suitable measurement sensors for Pulse Transient Time Measurement. The simplified block diagram of the IC is shown in Figure 3.3: MAX86150 ECG&PPG Sensor Block Diagram.

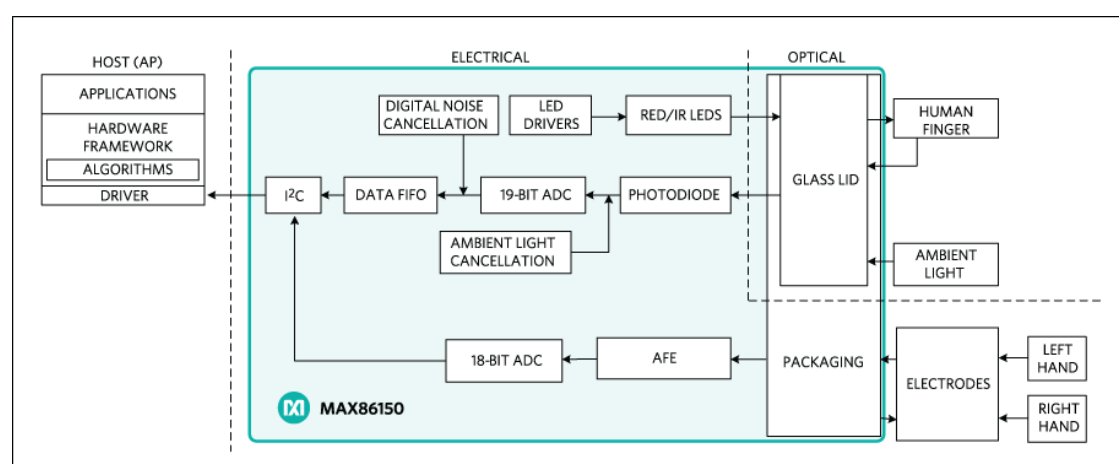


Figure 3.3: MAX86150 ECG&PPG Sensor Block Diagram [33]

3.4. MAX86150 (PPG&ECG) Integrated Circuit Sensor Evaluation Kit

Evaluation includes MAX86150 sensor IC, MAX32630 microprocessor, left and right finger ECG pads, analog, and digital i/o pads. MAX32630 is an arm-based microprocessor and acts as a host microprocessor for the sensor IC. The power of the sensor IC is also supplied from MAX32630FTR power output so that the power of the sensor IC is always stable. The evaluation kit is initially designed to use with square ECG pads by placing middle fingers on top of them and placing the index finger on the sensor to acquire PPG. The example usage can be seen in Figure 3.4.

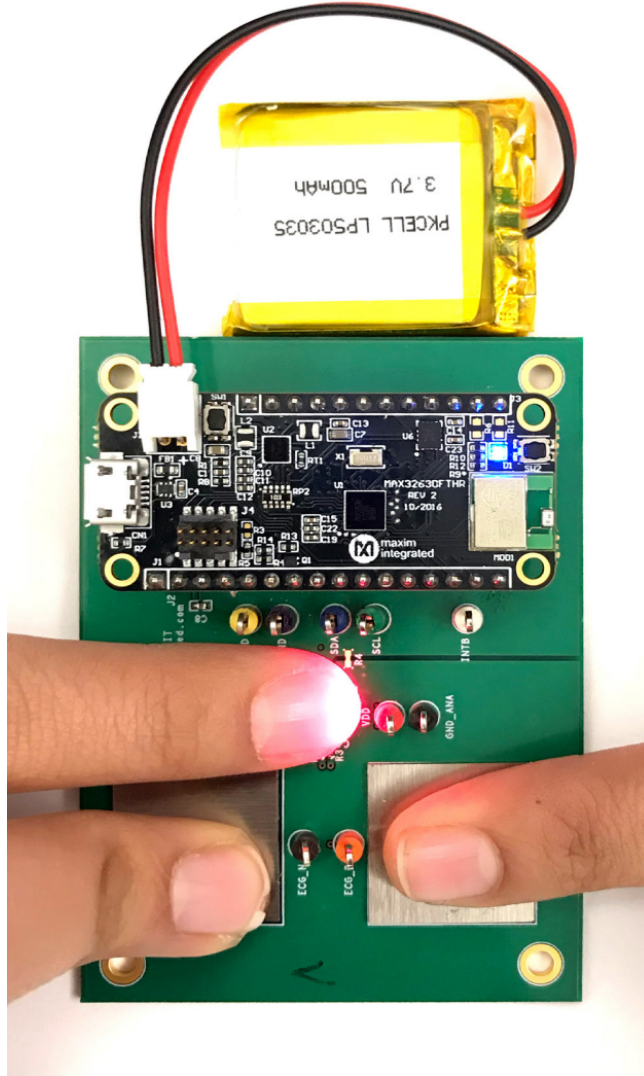


Figure 3.4: Typical finger placement for ECG&PPG measurement on MAX86150 Evaluation Kit [34]

However, that type of usage is not suitable for the data acquisition system. The i/o pads on the evaluation kit allow soldering external ECG cables. Hence, three ECG cables are soldered to the evaluation kit to have more comfort in the recording sessions. The soldered cables are for the right arm, left arm ECG, and analog ground. Soldering ECG pad compatible cables also increased the signal to noise ratio of ECG signal by using electrodes with impedance matching jell installed. ECG pad placements can be seen in *Figure 3.5*.

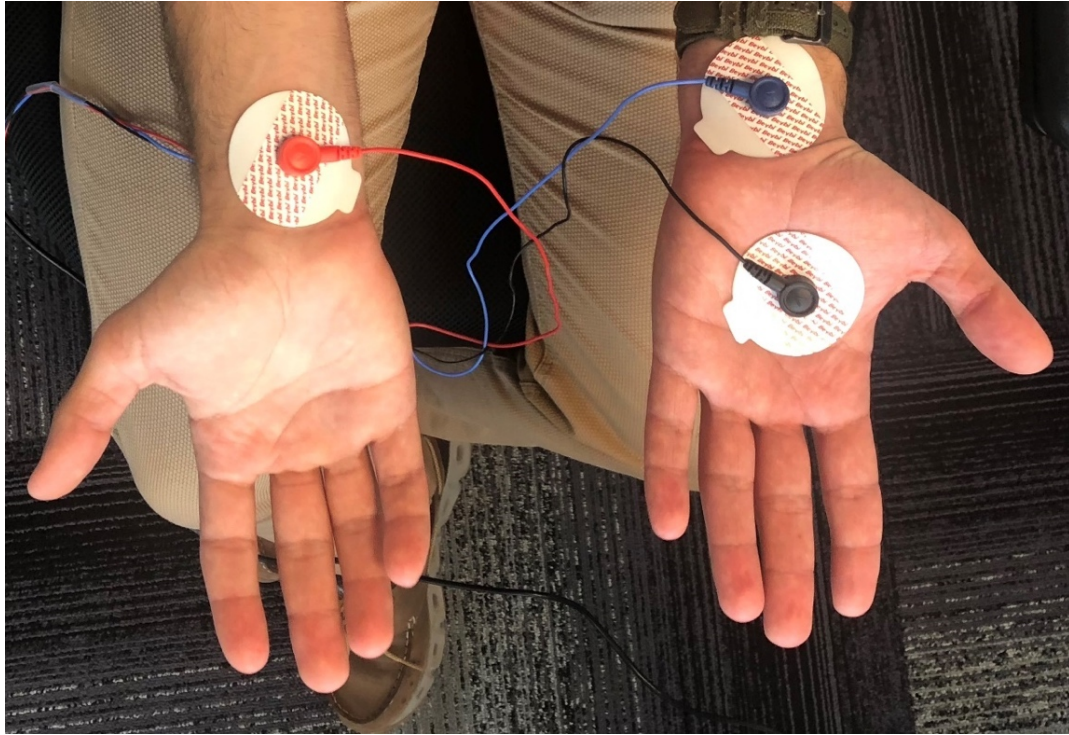


Figure 3.5 ECG Pad Placements: Red, Blue and Black corresponds to Left Arm, Right Arm and Analog ground respectively.

3.5. MAX86150 Sensor Evaluation Kit Software

Maxim Integrated Inc. releases user-friendly Evaluation Kits and lots of supporting documents to speed up the development process for its products. The evaluation kit software is downloaded from the website. The GUI connects to the evaluation board via Bluetooth and USB Serial port. To transfer acquired data USB serial is being used. Bluetooth connection is only for debugging purposes. There is also a very beneficial feature that GUI has. It shows the sensor IC's data stream in real-time. The software allows its users to select sampling frequency, PPG sensor currents, and ECG gain parameters. By looking at real-time data, the signal quality can be improved by changing user-selectable configurations. These settings are uploaded to the sensor IC when the GUI sent start monitoring command to the IC. On the *Figure 3.6* the screenshot of the GUI can be seen. On the left side, there are user-selectable parameter input boxes, on the right side, there are graphs that show real-time ECG and PPG data. While acquiring the experimental data, the user-configurable parameters such as gain,

and PPG LED drive current is adjusted for each subject at the beginning of the sessions to get better signal quality. During the exercise sessions, ECG pads may lose their stickiness, which results in corrupted signal. To overcome that ECG pads of the users are changed with new ones by examining the first instances of the data recordings thanks to GUI's real-time monitoring graphs.



Figure 3.6: MAX86150 Evaluation Kit Software Screenshot

3.6. High Speed RGB Video Camera

It has been shown in the studies that blood volume changes can be detected using video imaging [12], [15]. Poh et al. were used the ICA method to extract PPG signal from the subject's face and demonstrated that contactless real-time PPG measuring is possible by a simple webcam camera. In this thesis, the main aim is not only extracting PPG but measuring PTT. Therefore, the camera selection is a critical factor for this study. It was reported that PTT values between finger to face changes from 9.9 milliseconds to 99 milliseconds [20]. The sampling theorem states that the signal should be sampled at a frequency of $2F_0$, where F_0 is the maximum frequency the signal contains. To be able to measure 9.9 milliseconds of delay, the camera should capture frames with a period of 5 milliseconds. It is equal to 200 frames per second (FPS). To be on the safe side, by considering environmental noises that affect the video recording the frame rate requirement is set to 400 FPS.

To acquire high resolution video or sequential images market search was conducted. There were seven main requirements to be fulfilled.

- 1- It should capture frames at least 400Hz to have 2.5 millisecond of resolution.
- 2- It should have enough resolution to cover whole face of a person.
- 3- It should record in RGB color space to get better video PPG extraction.
- 4- There should be an application program interface (API) for the camera to get recording without need for extra data processing.
- 5- It should record at least a minute of data continuously.
- 6- It should not be so expensive.
- 7- It should record frames in RAW format to assure no data loss.

First, smartphone cameras are considered, there are plenty of smartphones that can be capable of recording a video at higher frame rates (up to 960 FPS.) However, none of them can record a video higher than 240 Hz for a minute. Then, action cameras are searched to find any suitable one. Similarly, none of them can record a minute of data with sample rate higher than 240 FPS. Lastly, industrial cameras were considered and

found a suitable one. Basler Ace 720-520uc (Figure 3.7) is selected as an RGB high-speed camera. Its features are listed as follows.

- It captures up to 525 RGB frames per second
- Frame capture can be triggered externally by using GPIO pins
- Have resolution of 720 by 520 pixel
- Costs only around 500 USD including C-Mount lens and USD cable.
- Basler (manufacturer) provides free API for both Windows and macOS PCs to download captured frames from the camera.

All of these features make the camera excellent choice for the experimental data acquisition setup.



Figure 3.7: Basler Ace 720-540uc Video Camera

3.7. IC Sensor Data and Video Camera Data Synchronization

Video cameras and IC sensors are not linked by their internal clocks. Therefore, there was a need for a synchronization method to perfectly sync the data streams coming out of them to measure pulse transient time correctly. Comparing time stamps of the recordings can be considered to be a good synchronization method. However, the PC's operating systems are not real-time systems. Their timestamps are not a reliable source of information even though they are in sync through Network Time Protocol (NTP) servers. Especially if there is high throughput output data present, the accuracy of the timestamps decreases realistically. To overcome this problem, a synchronization method using LED is proposed.

3.7.1. Sync Using a LED Placed within the Recording Frame

MAX86150 IC on the evaluation kit is driven by MAX32630 host microprocessor. Firmware of the microcontroller is tweaked to produce a unique PWM waveform from one of its digital pinouts, at the instant of data recording starts. The period of the PWM cycle is eight seconds. The duty cycle of the waveform is 1/32. The pinout is connected to a Red-colored LED. When data recording is started by evaluation kit GUI, the microprocessor sends the start command to sensor IC to start collecting data. Right after that, it initiates the PWM waveform from one of its pinouts. Therefore, at the instant of MAX86150 starts to acquire data from PPG and ECG analog end, LED starts to blink with the same duty cycle. The example of the produced PWM waveform can be seen in Figure 3.8.

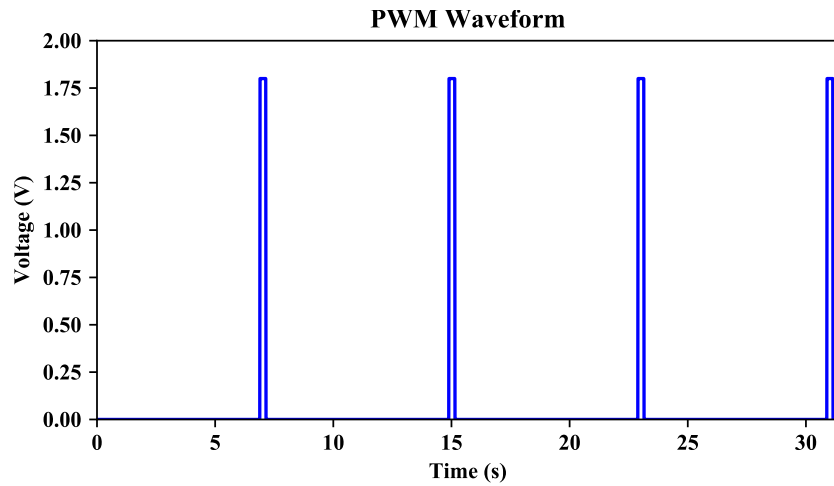


Figure 3.8: Produced PWM waveform

The LED is placed at the backside of the subjects. The position of the LED is aligned for every session to make sure that it is in the field of view of the recording camera. Every time data acquisition is started from MAX86150 Evaluation Kit GUI software, the LED is observed by the eye. Once, the LED blinks the first time the video camera recording is started. By doing so, the camera captures the first blink of the LED when exactly 8 seconds have passed from the instant when the sensor IC starts to acquire data. The LED which is placed right behind the subject can be seen within the blue square in Figure 3.9.



Figure 3.9: LED Placement

CHAPTER 4

DATA PROCESSING

The data processing scheme is represented in Figure 4.1. Each block of the data processing will be detailed in the following sections. Due to the high throughput of the video-image stream coming out from the camera, a MacBook Pro with an SSD hard drive is selected as a recording end due to its higher performance over most of the PCs on the market. On the other hand, Maxim doesn't release macOS version of the Device Studio (MAX86150 Evaluation Kit Software). Therefore, a Dell ThinkPad PC is used to run and acquire data coming out of the MAX86150 Evaluation Kit. The output data of the MAX86150 is stored in CSV format.

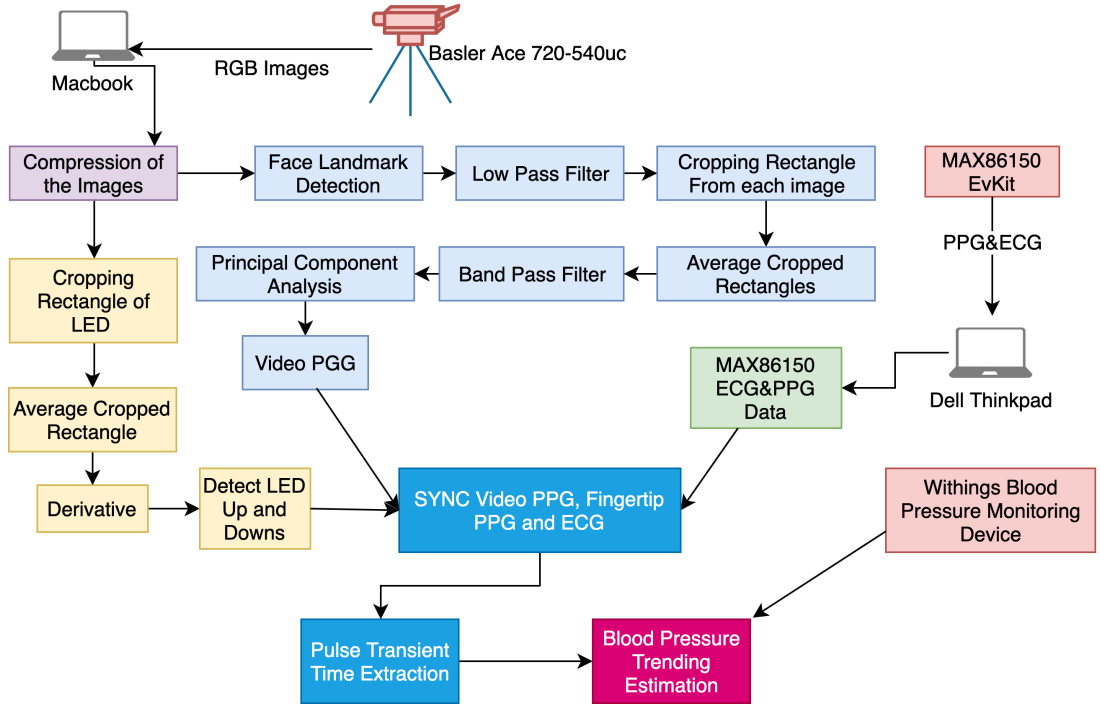


Figure 4.1: Data Processing Scheme

4.1. Handling Output of High-Speed Camera

As detailed in the previous sections, the camera records 400 RGB 8-bit images per second in Tagged Image File Format (TIFF), RAW format. The recorded images have 720 by 540 resolution. The single image occupies 1.112 Mbytes of storage ($720 \times 540 \times 3$ bytes). As a result of that, if the recording duration is about to a minute, approximately 26.06 Gigabyte ($(1.112 \times 400) \times 60$ Mbytes) of data will be recorded. Processing that amount of data is cumbersome, there should be a method to shrink the size of the data without compromising the information stored in the images. There are some options to decrease the size of the images. They can be categorized into two as lossy and lossless image compression techniques. Not to lose information, lossless compression techniques should be used. After a little bit of research, Portable Network Graphics (PNG) lossless compression is selected. Because it is free to use and supported by lots of python libraries. After each data recording session, which includes four different stages, there were ~100 Gigabytes ($27 \text{ Gigabytes} \times 4 \text{ sessions}$) output data of camera recording. And they were recorded 90-degree clockwise rotation to cover the whole face. Each recorded image is rotated -90 degree back and compressed to PNG format from TIFF by using multiprocessing to increase CPU utilization. The process decreased the image size to almost 1/3 percent of its RAW format size without having any loss of information. Therefore, 2/3 percent of the storage is saved. There is also another benefit of the decreasing size of the image. The data reading time from memory highly depends on their types. By considering today's technology, the PC's random-access memories (RAMs) are always faster than their hard drives. Reading a single PNG image from the hard drive is three times faster than reading the TIFF image. Once the PNG image is read, it will be stored at the RAM and uncompressed. Uncompressing is handled by CPU while compressed one is present at the RAM. Reading and uncompressing PNG image is faster than only reading uncompressed TIFF image if there were thousands of reading operations as in this case.

4.2. Detecting Face Landmarks

Face detection is one of the most used applications of computer vision. There are lots of pre-trained libraries to detect faces in the input images. Some of them can also detect facial landmarks to segment face to facial parts such as lips, eyes, and nose. Most of the previous studies which extract PPG from video recording have used OpenCV's built-in face detection and segmentation method [12], [15]. The method is based on Haar feature-based cascade classifiers, proposed by Viola et al. [35]. It has some disadvantages as follows. It is an old method, and doesn't have good enough accuracy if there is not any tracking algorithm runs with the detection to correct the algorithm's erroneous face detection and localization. It highly tends to produce garbage detections. Its face segmentation is also so primitive. Hence, it is decided to use one of the most recent face algorithms which would have good accuracy and ability to detect multiple face segments. Detecting multiple face landmarks may allow extracting multiple PPG waveforms from the video recording from different locations of the face such as forehead and cheeks. Most recent face detection algorithms are compared and found a suitable one for this study. A 68-point shape detector is used from the Dlib Library [36] to detect face landmarks. Dlib library is a machine learning library written in C, C++ to have one of the best performances among Python machine learning libraries. Amount of the camera data to be processed effects the performance. So, performance criteria were also one of the most important criteria when selecting a face detection algorithm. Moreover, it has more face landmarks than most of the face landmark detection algorithms. That allows selecting a rectangular region of the forehead and track it more preciously than simple face feature detection algorithms used in the previous research papers. The landmarks are seen as green dots placed on top of a subject's face in Figure 4.2. For each frame of the video recordings, face and facial landmarks are detected. Thanks to its high accuracy, tracking algorithms were not needed and used.

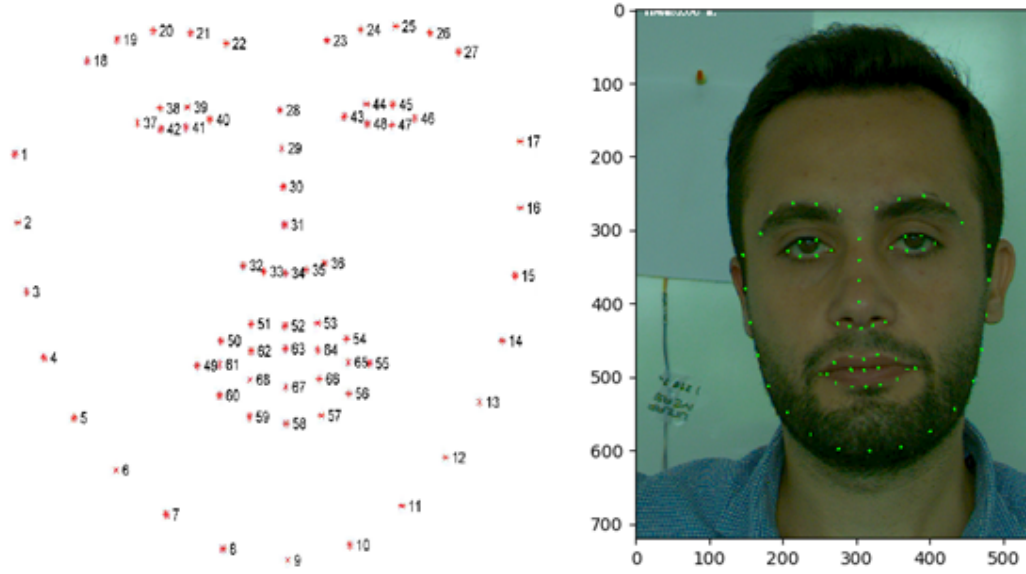


Figure 4.2: Detected Facial Landmarks

4.2.1. Applying Moving Average Filter to Face Landmarks

The subject's head is always moving slightly during the video recording sessions. Even though they are trying to stand still, the cardiac cycle creates slight movements when the heart pushes the blood the face. From these movements, another PPG waveform can be extracted, but that method hasn't been used in this thesis [37]. The face detection algorithm also has its own spatial error. The slight head movements and face detection algorithm's error accumulates and creates high-frequency vibrations on the detected face landmark points. Those high-frequency vibrations need to be suppressed to get a better signal to noise ratio of PPG waveform from the video. Therefore, a moving average filter is applied to detected face landmark points. Moving average filter is a low pass filter. It decreased the high-frequency components of the vibrations. Detected coordinates of one of the facial landmarks before and after moving average versus time plot can be seen in Figure 4.3 and Figure 4.4.

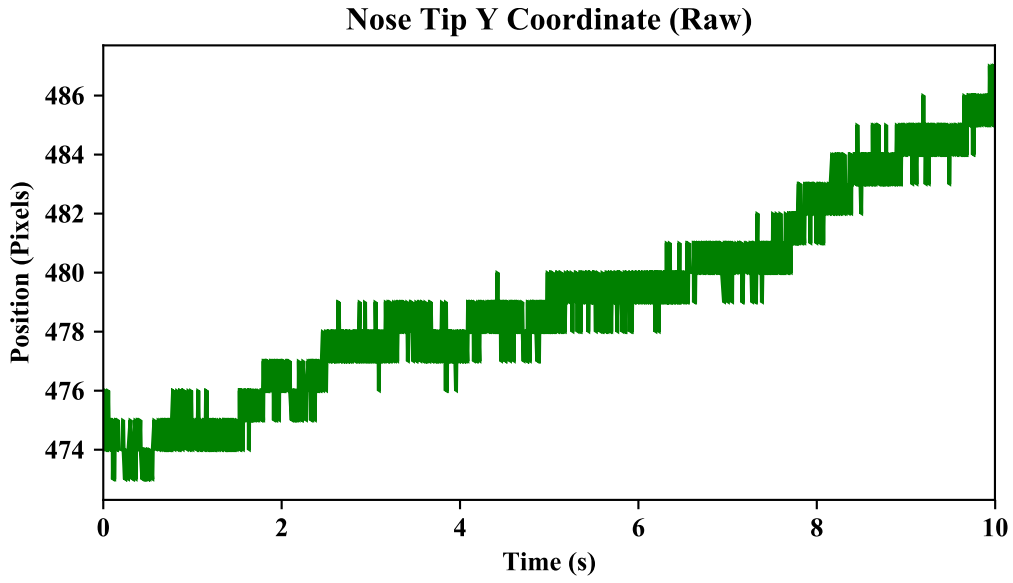


Figure 4.3: Y-Coordinate of one of Facial Landmark

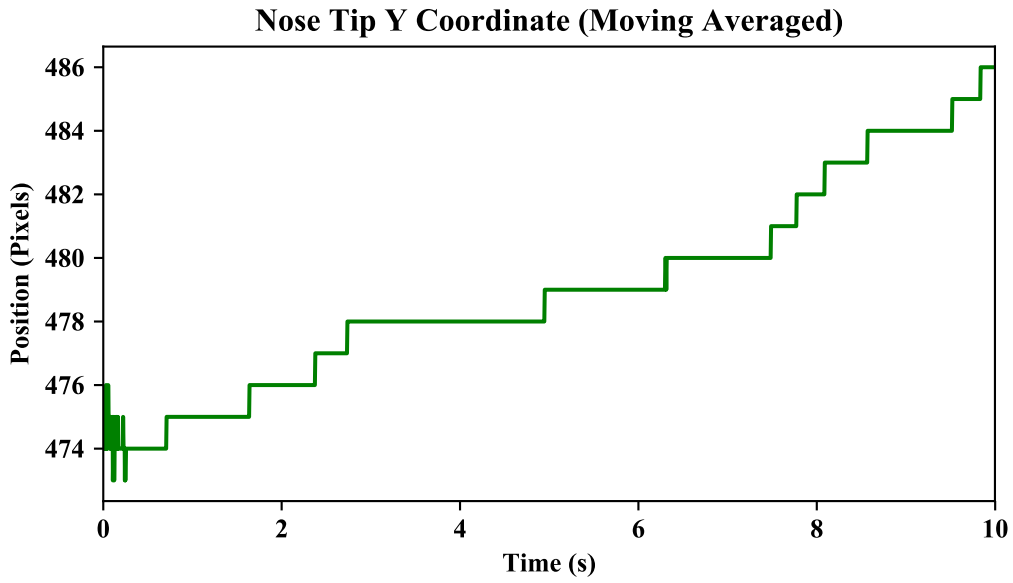


Figure 4.4: Y-Coordinate of one of Facial Landmark after moving average filter applied

4.3. Cropping a Rectangle Frame from the Subject's Face

Detecting face landmarks as detailed in the previous section allows cropping rectangles from the face. Each face segment has its advantages and disadvantages to be used for PPG extraction. The forehead is one of the best segments to be used

because it is not covered by the beard and has a wider area among the face segments. So, in this study, a cropped rectangle from the forehead is segmented from the subject's face. Then, it has been used to extract video PPG waveform. Rectangle was positioned as follows. Five landmarks placed on each eyebrow create a concave line on the eyebrows by the face detection algorithm mentioned in the previous section. The points numbered as 20 and 25 are used to draw the bottom line of the cropped rectangle. From the subject to subject, forehead area is changing. Some has wider forehead than others. The area of the rectangle was adjusted according to the subject's forehead width in order to not to include any area other than forehead of the subjects. The height of the rectangle was also adjusted to fit into the forehead area. By doing so, the frontal hair of the subject is also excluded from the cropped rectangle, to get a better signal to noise ratio. The yellow area in *Figure 4.5* shows cropped rectangle.

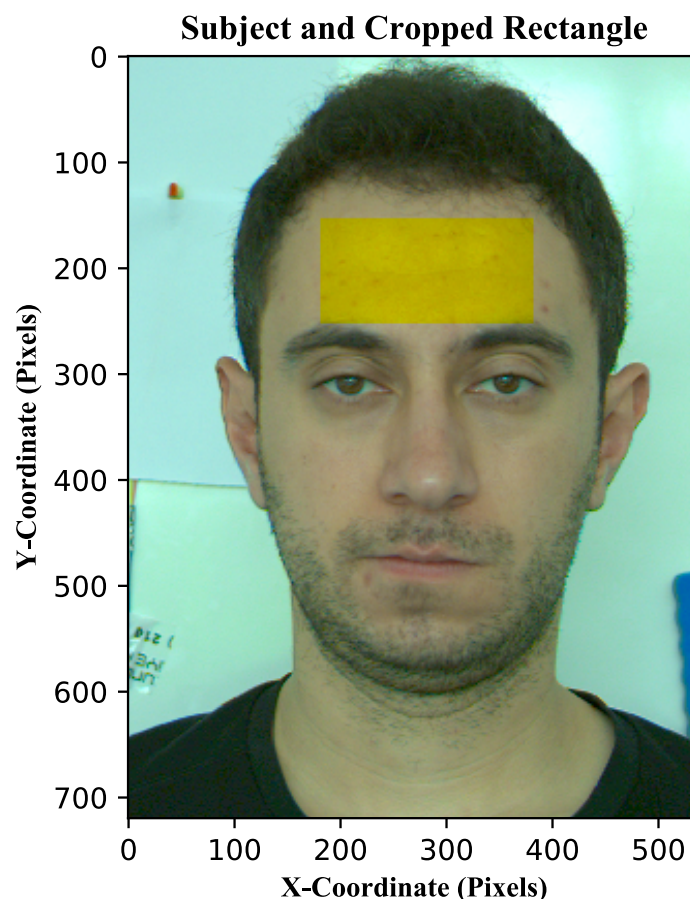


Figure 4.5: Cropped Rectangles

4.4. Averaging the Cropped Rectangle and Bandpass Filter

It is known that cropped rectangle stores information about the blood pressure pulse wave. However, there are lots of noise introduced to the pixel values at the cropped rectangle. The major ones can be listed as small illumination changes in the room where the subject sits, the angle of illumination, the factors that create skin color differences on the face, the camera's internal noise as the temperature of its sensor changes slightly over time. To suppress the noise coming from multiple sources, the average value of the cropped rectangle was calculated. Therefore, for each RGB channel, a one-dimensional time-domain signal is obtained. It is known that for a healthy adult, the heart beats 45 to 240 per minute. So, the time domain signal was fed into a bandpass filter having cut off frequencies as 0.75 Hertz to 4 Hertz to eliminate signals having lower or higher frequency than frequency interval of heart rate. The raw signals can be seen in Figure 4.6, and filtered signals can be seen on the Figure 4.7.

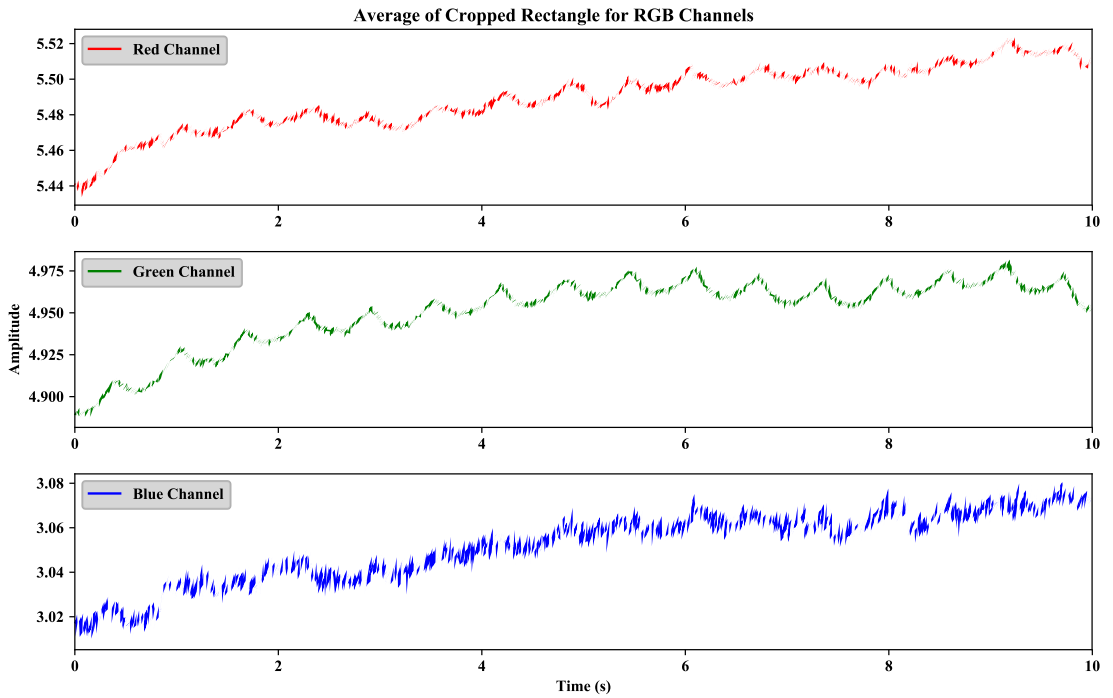


Figure 4.6: Raw signal of RGB channels of Average of Cropped Rectangle

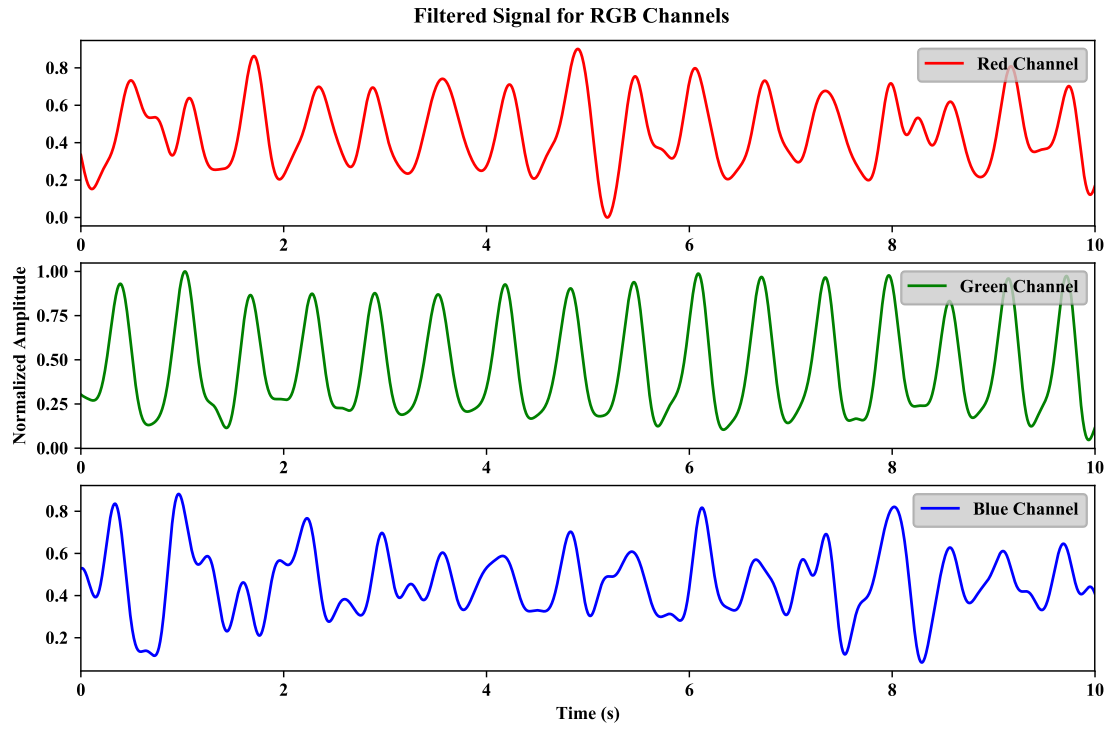


Figure 4.7: Bandpass Filtered Signals

4.5. Applying Principal Component Analysis

Bandpass filter output gives RGB channel waveforms. As it is seen in Figure 4.7, the green channel is much more sensitive to blood pressure changes than the others. It is also shown in previous studies [16]. But, previous studies showed that red and blue channels also have information about blood pressure changes in the skin [14]. Therefore, a dimension reduction technique which is Principal Component Analysis is applied to the waveform to get a single-channel waveform from the RGB channels. Finally, video PPG waveform is obtained. The resulting waveform can be seen in Figure 4.8.

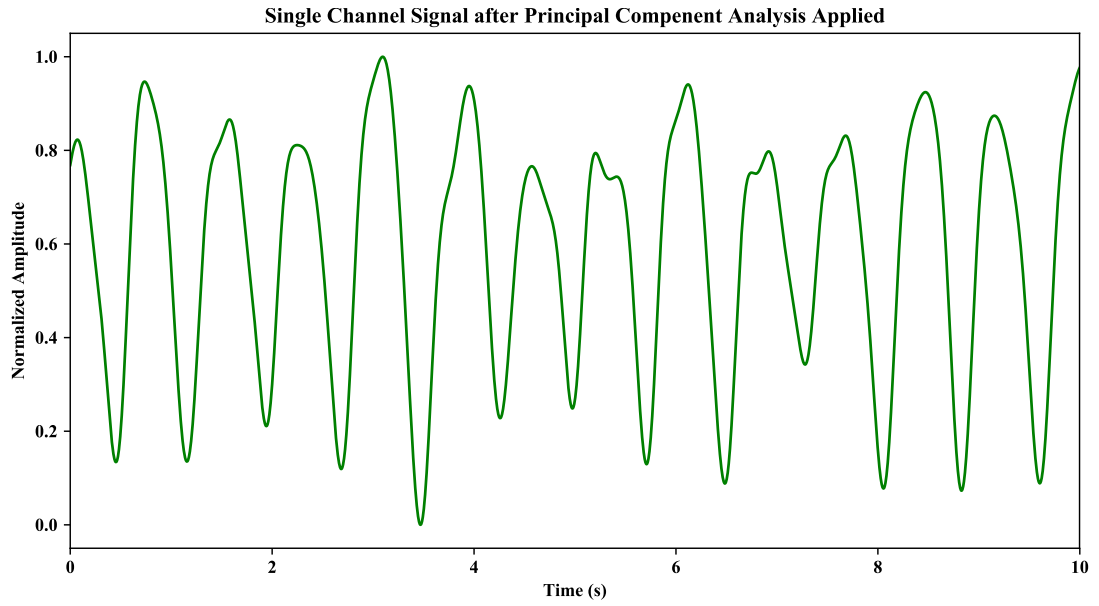


Figure 4.8: Video PPG waveform

4.6. Calculating Time Difference Between Video and IC sensor Recordings

It has been mentioned in the previous sections that video and the IC sensor recordings aren't in synchrony. They need to be synchronized by using a method that transfers a piece of information to the other. To achieve perfect symbolization, a Red-colored LED is blinked with a Pulse Width Modulation (PWM) waveform. The PWM waveform has a duty cycle of 1/32 and 8 seconds of a period. The PWM is initialized at the beginning of the IC sensor recording. And, the camera has always started the recording right after the first LED blink is seen by an observer. Therefore, the time when the camera captured the first blink, the LED will indicate the time difference between the first instances of the data streams. To detect first blink in the recording frame, the coordinates of the LED is found by examining the first frame of the video recording for each subject. Then based on these coordinates, a rectangle includes only the LED is cropped from each frame. The cropped frame is averaged, and only the red channel is extracted to get a one-dimensional signal. The signal can be seen in Figure 4.9.

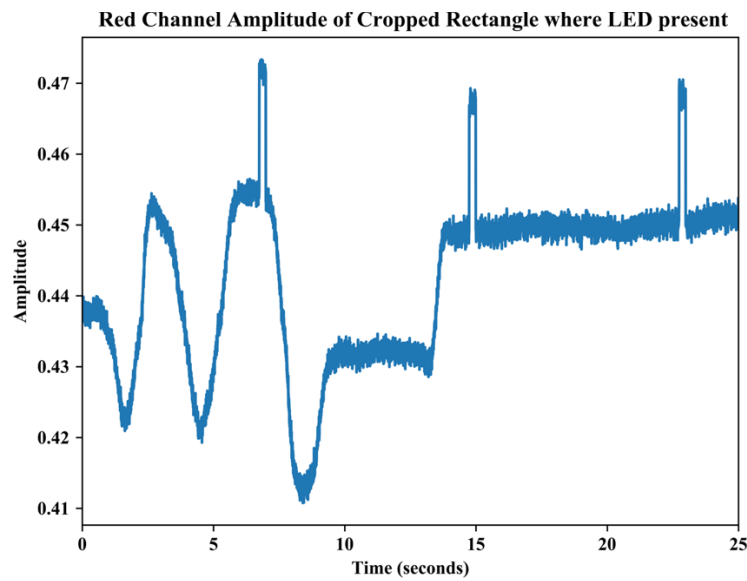


Figure 4.9: Red Channel Signal of Cropped LED Area

To find out the exact points where LED blinks, the derivative of the signal is calculated. The resulting signal can be seen in *Figure 4.10*. Then, the average of the derivative signal is calculated and searched for the points which are greater than the mean of average and the maximum value of the signal. Finally, the time instants where the LED blinks are found.

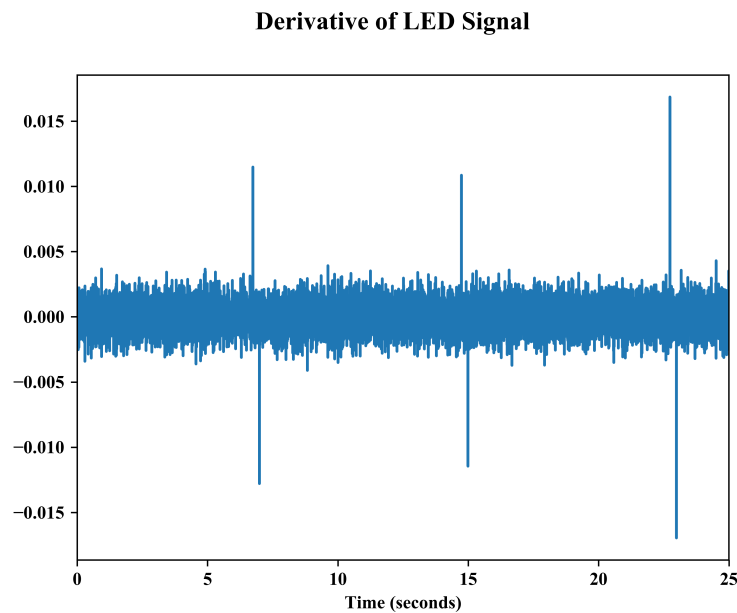


Figure 4.10: Derivative of LED Signal

4.7. Removing Baseline from the Recorded Signals

Both ECG and PPG signals have small oscillations due to environmental noise such as movement artifacts, sensors' internal noise. These summed up and added to these signals as an oscillating dc baseline. That baseline needs to be removed from the signals to get better accuracy for further processing. There are several methods to use to remove the baseline. These methods require filters to be applied. The most common ones are Kalman filter, high pass filter, and The Savitzky–Golay filter. The Savitzky–Golay filter has advantages over the others because it doesn't need any parameter than filter width and doesn't distort the signal as high pass does [38]. Therefore, the signals fed into The Savitzky–Golay filter to get the waveform of baseline. Then, the baseline waveform is subtracted from the original signal. Finally, oscillations are eliminated from the ECG and PPG signals. Original and baseline removed versions of the signal can be seen in Figure 4.11 and Figure 4.12.

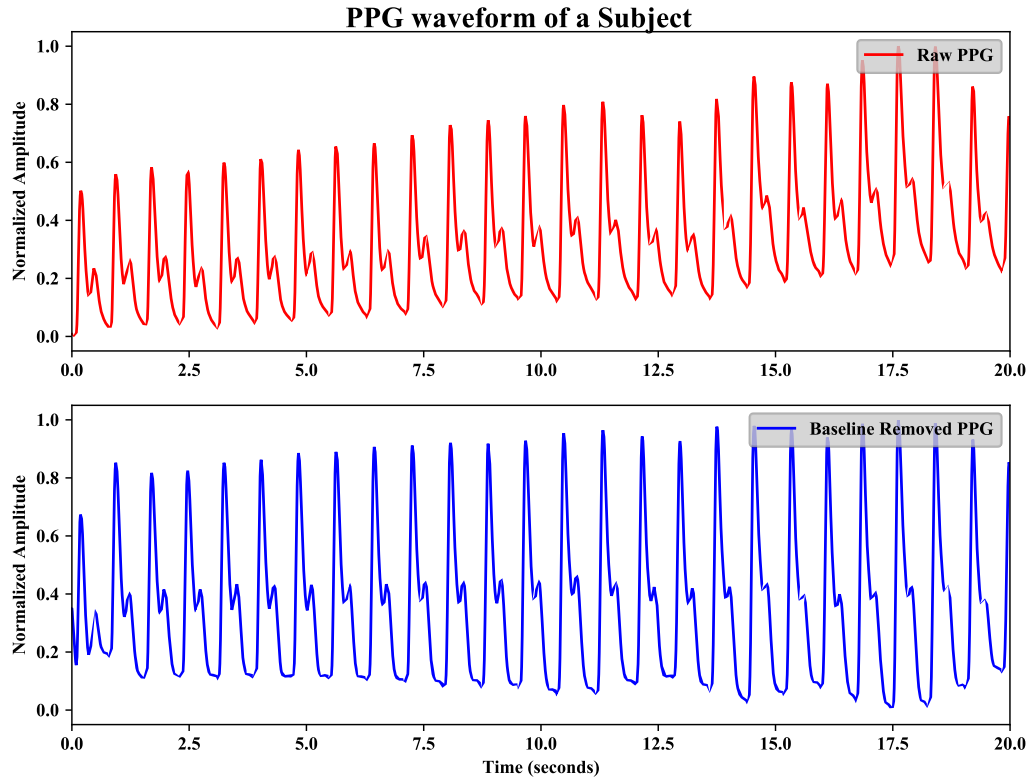


Figure 4.11: PPG waveform before and after Baseline removed

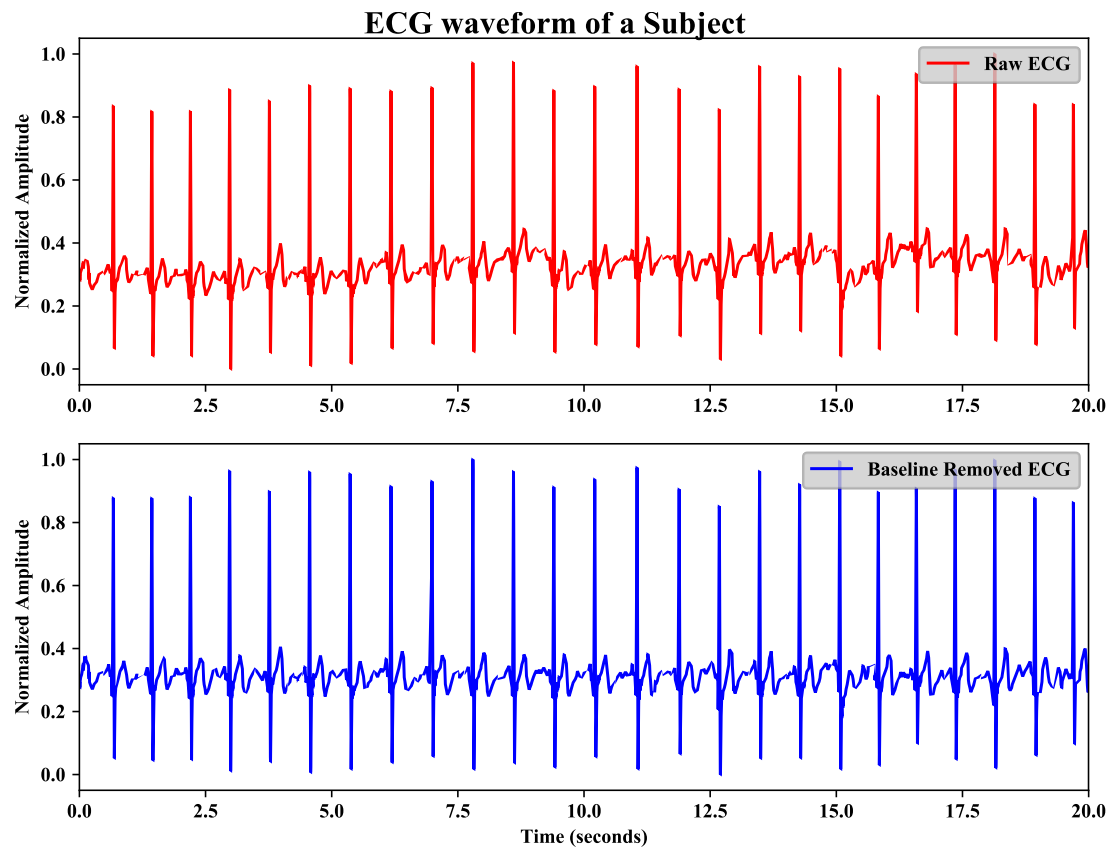


Figure 4.12: Baseline Removed ECG

4.8. Pearson Correlation Coefficient (r)

The correlation coefficient is a statistical term that is used to measure the linear relation between two variables, and it is widely used in statistics. Since it is widely used, there are various types of correlation coefficients. The most common one is the Pearson Correlation Coefficient, which is denoted by “ r ”. The value of r changes from -1 to 1. It represents strength of correlation of variables. While 1.0 represents a perfect positive correlation between two variables, -1 presents a perfect negative correlation. Positive correlation implies, both variables increase or decrease together as the value of one of them changes. On the other hand, negatively correlated variables move in opposite directions, for a positive increase in the one, there should be a decrease for the other, for the negative increase vice versa. The value of 0 indicates the variables

are completely independent of each other. The coefficient r is calculated for paired series of variables $[(x_1, y_1) \text{ to } (x_n, y_n)]$ consisting n pairs by using Equation 1.

$$r_{x,y} = \frac{\sum_{i=1}^n (x_i - \bar{x})(y_i - \bar{y})}{\sqrt{\sum_{i=1}^n (x_i - \bar{x})^2} \sqrt{\sum_{i=1}^n (y_i - \bar{y})^2}} \quad (1)$$

where:

- n is number of pairs
- x_i, y_i are the individual points
- \bar{x} and \bar{y} mean of series of \bar{x} and \bar{y}

Example plots of x and y series of variables and their Pearson Correlation Coefficients can be seen in *Figure 4.13*, *Figure 4.14*, and *Figure 4.15*

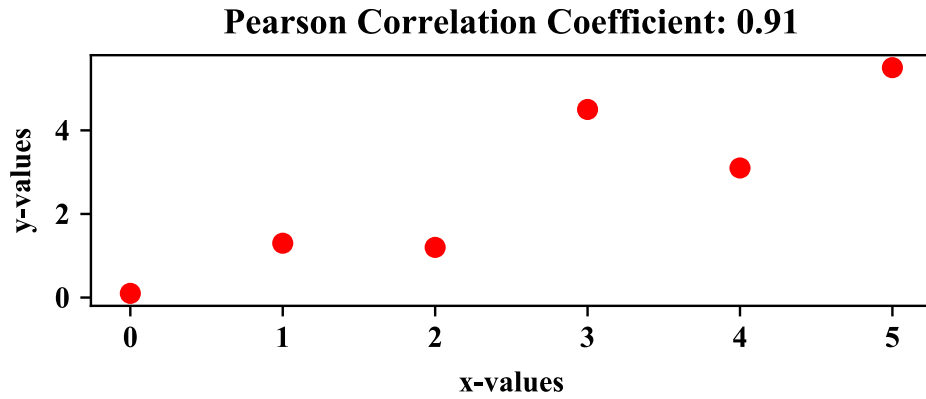


Figure 4.13: Positive Strong Correlation

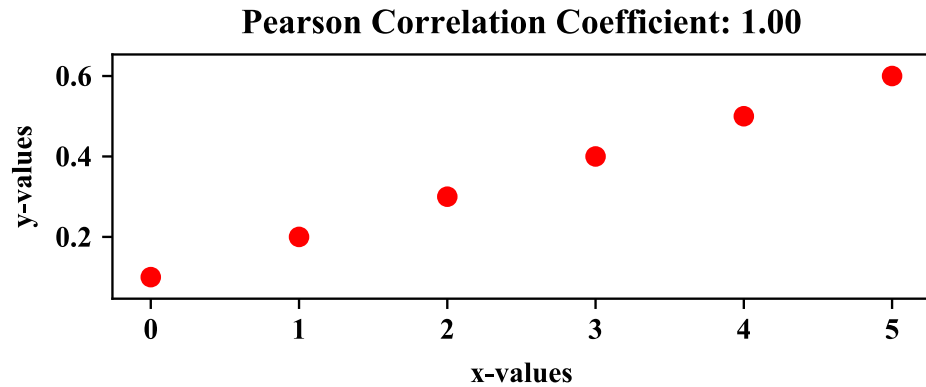


Figure 4.14: Positive Perfect Correlation

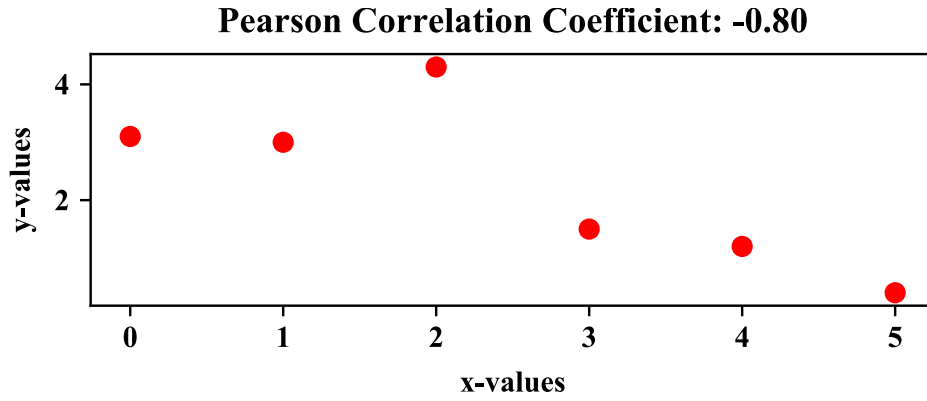


Figure 4.15: Negative Strong Correlation

Pearson Correlation Coefficient is used to investigate the relation between PTT and BP to enable BP trending estimation. It is the latest step of the data processing steps. After video recordings are processed, rPPG waveforms are extracted. PTT values are calculated by using rPPG, contact PPG, and ECG waveforms. These steps have been done for each subject, and each session separately. Then, Pearson Correlation Coefficients are calculated for PTT and BP pairs for each subject.

4.9. Spearman's Rank Correlation Coefficient (r_s)

Spearman's Rank Correlation Coefficient is nonparametric measure of the strength of a monotonic relationship of two variables. Strength of the correlation is denoted by " r_s " and changes from -1 to +1 similar to similar to Pearson's correlation coefficient " r ". Unlike Pearson's correlation coefficient, Spearman's correlation coefficient doesn't require normality of the data. Therefore, it is nonparametric statistics and it is better to use if the data set is small. Positive value of " r_s " represents the two variables monotonically increasing, negative value of " r_s " represents the two variables monotonically decreasing. The coefficient " r_s " is calculated for series of variables $[(x_1, y_1) \text{ to } (x_n, y_n)]$ consisting n observations by using Equation 2.

$$r_{s_{x,y}} = 1 - \frac{6 \sum d_i^2}{n^3 - n} \quad (2)$$

where:

- $d_i = rg(X_i) - rg(Y_i)$ difference between ranked pairs
- x, y are observation vectors
- n is the number observations

Spearman's Correlation Coefficient is used to investigate the monotonic relationship between PTT and BP.

CHAPTER 5

RESULTS

5.1. Subject Characteristics

In this thesis, ten subjects have participated in experimental data collection sessions voluntarily. They are six male and four female, and their ages, heights, and weights are ranging from 21 to 30 years, 164 to 181 cm, 56.0 to 88.3 kg, respectively. Characteristics of the subjects can be seen in Table 1.

Table 1: Characteristics of Subjects

<i>Subjects</i>	<i>Gender</i>	<i>Age (years)</i>	<i>Height (cm)</i>	<i>Weight (kg)</i>
1	Male	30	181	82.0
2	Female	28	164	62.3
3	Male	30	172	83.3
4	Male	28	176	67.0
5	Female	21	168	56.0
6	Male	29	178	88.3
7	Male	27	171	66.2
8	Female	24	168	57
9	Female	25	165	63
10	Male	27	170	66

5.2. Blood Pressure Measurements of the Subjects

As detailed in the data collection setup, subjects' blood pressure are measured by a gold standard measurement device for each session. In addition to that mean arterial blood pressure (MAP) is calculated based on Equation 2 [39]. These measurements for each subject can be seen in Table 2.

$$MAP = \frac{2DBP + SBP}{3} \quad (3)$$

5.3. Pulse Transient Time Varieties

There are different kind of pulse transient time measurements in the literature. They differs with respect to the points that selected as arrival of pulse [31]. Generally, PTT is calculated as time interval between ECG-R wave and first maximum point of first derivative of PPG waveform or the first maximum point of PPG waveform of the same cardiac cycle. In this study, there are two PPG signals. One is contact fingertip PPG, the other is Video PPG. For two of them there are four different PTT calculations as follows:

- difference between PPG maximum and ECG-R wave, PTT1
- difference between first derivative of PPG maximum and ECG-R wave, PTT2
- difference between Video PPG maximum and ECG-R wave, PTT3
- difference between first derivative of Video PPG maximum and ECG-R wave, PTT4

Points used for PTT calculations can be seen on the *Figure 5.1*. Blue dots on the ECG waveform represents ECG R waves. Orange stars on PPG waveforms represents maximum of the derivative of the corresponding waveforms. Green stars represents the maximum point of the PPG waveforms.

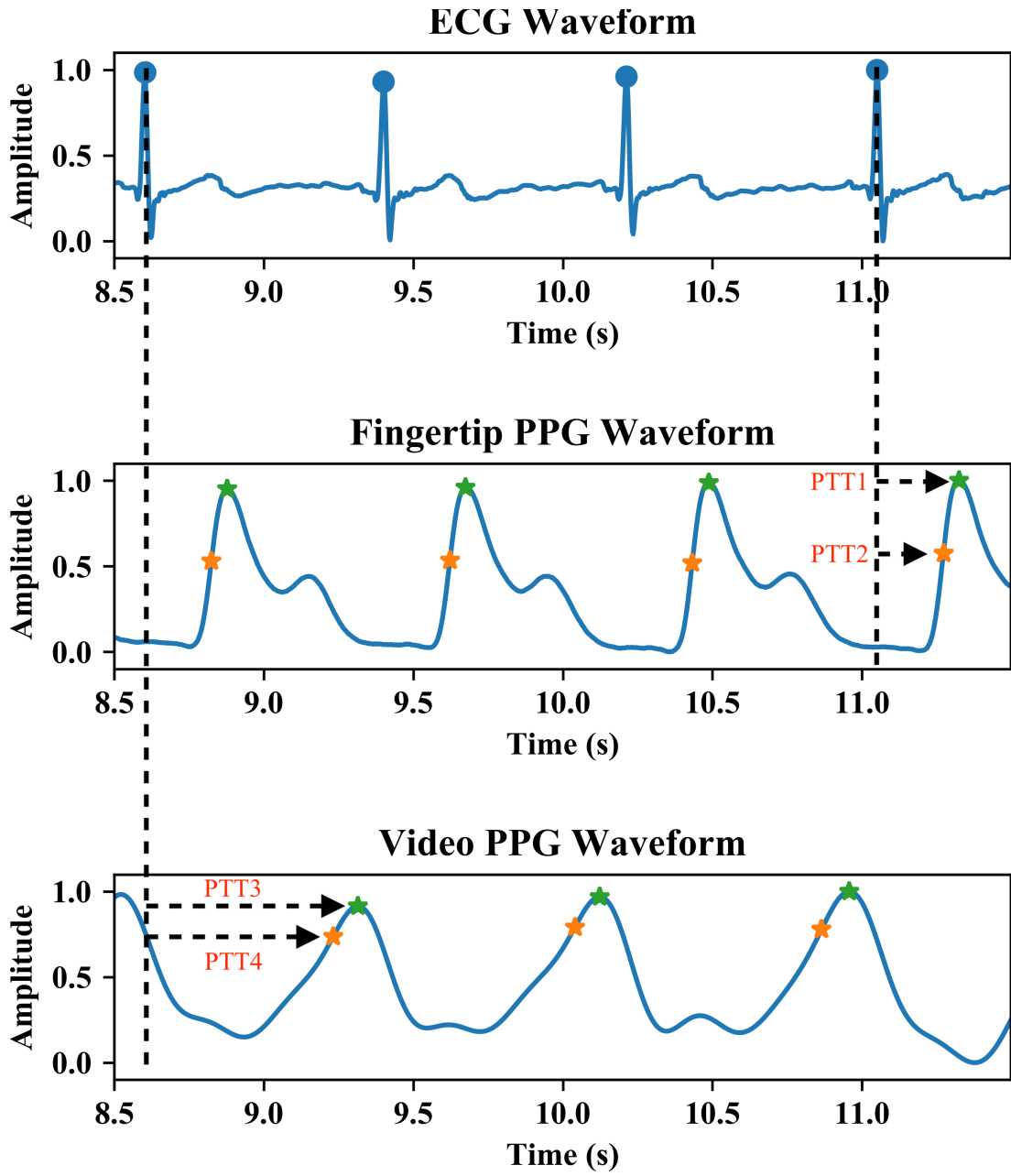


Figure 5.1: PTT calculation

In order to find relationship in between BP and PTT as explained previously, four different PTT values are calculated for each subject and session. PTT values and BP measurements can be seen at Table 2.

Table 2: Blood Pressure and PTT measurements for each subject, session

		<i>Sessions</i>			
<i>Subjects</i>		<i>Rest 01</i>	<i>Exercise 01</i>	<i>Rest 02</i>	<i>Exercise 02</i>
1	SBP (mmHg)	104.00	120.00	110.00	120.00
	DBP (mmHg)	73.00	80.00	74.00	73.00
	MAP (mmHg)	83.33	93.33	86.00	88.67
	PTT1 (sec)	0.28	0.26	0.30	0.25
	PTT2 (sec)	0.22	0.21	0.22	0.18
	PTT3 (sec)	0.73	0.51	0.70	0.12
	PTT4 (sec)	0.64	0.23	0.61	0.59
2	SBP (mmHg)	92.00	105.00	99.00	106.50
	DBP (mmHg)	63.00	61.00	66.00	67.50
	MAP (mmHg)	72.67	75.67	77.00	80.50
	PTT1 (sec)	0.53	0.26	0.28	0.25
	PTT2 (sec)	0.20	0.19	0.21	0.18
	PTT3 (sec)	0.26	0.32	0.35	0.58
	PTT4 (sec)	0.78	0.28	0.02	0.46
3	SBP (mmHg)	119.50	145.00	129.00	140.50
	DBP (mmHg)	80.00	88.00	91.00	89.50
	MAP (mmHg)	93.17	107.00	103.67	106.50
	PTT1 (sec)	0.24	0.23	0.26	0.20
	PTT2 (sec)	0.17	0.15	0.18	0.14
	PTT3 (sec)	0.58	0.12	0.50	0.08
	PTT4 (sec)	0.48	0.65	0.36	0.53
4	SBP (mmHg)	109.00	128.00	115.00	135.00
	DBP (mmHg)	71.00	80.50	75.00	82.00
	MAP (mmHg)	83.67	96.33	88.33	99.67
	PTT1 (sec)	0.25	0.22	0.25	0.22
	PTT2 (sec)	0.20	0.17	0.19	0.16
	PTT3 (sec)	0.65	0.21	0.34	0.49
	PTT4 (sec)	0.53	0.03	0.07	0.39
5	SBP (mmHg)	121.00	139.00	116.00	121.00
	DBP (mmHg)	79.00	80.00	88.00	76.00
	MAP (mmHg)	93.00	99.67	97.33	91.00

	PTT1 (sec)	0.24	0.19	0.24	0.19
	PTT2 (sec)	0.18	0.14	0.18	0.14
	PTT3 (sec)	0.54	0.03	0.30	0.03
	PTT4 (sec)	0.44	0.42	0.18	0.38
6	SBP (mmHg)	132.00	131.00	129.00	136.00
	DBP (mmHg)	76.00	75.00	80.00	82.00
	MAP (mmHg)	94.67	93.67	96.33	100.00
	PTT1 (sec)	0.31	0.29	0.30	0.27
	PTT2 (sec)	0.23	0.21	0.22	0.20
	PTT3 (sec)	0.35	0.25	0.22	0.57
	PTT4 (sec)	0.12	0.37	0.05	0.41
7	SBP (mmHg)	117.50	126.00	116.00	131.50
	DBP (mmHg)	79.00	67.00	67.00	67.50
	MAP (mmHg)	91.83	86.67	83.33	88.83
	PTT1 (sec)	0.27	0.23	0.25	0.25
	PTT2 (sec)	0.20	0.17	0.19	0.18
	PTT3 (sec)	0.31	0.20	0.58	0.67
	PTT4 (sec)	0.46	0.06	0.40	0.53
8	SBP (mmHg)	101.00	125.00	106.00	128.50
	DBP (mmHg)	74.00	80.00	77.00	86.50
	MAP (mmHg)	83.00	95.00	86.67	100.50
	PTT1 (sec)	0.52	0.25	0.27	0.21
	PTT2 (sec)	0.22	0.18	0.20	0.15
	PTT3 (sec)	0.63	0.46	0.38	0.38
	PTT4 (sec)	0.40	0.42	0.24	0.26
9	SBP (mmHg)	106.00	132.00	112.00	132.00
	DBP (mmHg)	73.00	80.00	74.00	88.00
	MAP (mmHg)	84.00	97.33	86.67	102.67
	PTT1 (sec)	0.26	0.23	0.23	0.22
	PTT2 (sec)	0.17	0.17	0.17	0.15
	PTT3 (sec)	0.27	0.26	0.51	0.55
	PTT4 (sec)	0.35	0.80	0.43	0.45
10	SBP (mmHg)	122.00	142.00	126.00	145.00
	DBP (mmHg)	81.00	87.50	79.00	85.00

MAP (mmHg)	94.67	105.67	94.67	105.00
PTT1 (sec)	0.26	0.24	0.28	0.24
PTT2 (sec)	0.19	0.17	0.20	0.18
PTT3 (sec)	0.42	0.63	0.47	0.17
PTT4 (sec)	0.21	0.51	0.25	0.28

5.4. Blood Pressure and Pulse Transient Time Correlation

Linear correlation between BP and PTT's are investigated based on the Pearson Correlation Coefficient and Spearman Correlation Coefficient. Pearson Correlation Coefficient is a statistical method used to test strength of a linear association between two variables as detailed in Chapter 4. On the other hand, Spearman Correlation Coefficient is nonparametric correlation coefficient and used to test monotonic correlation. PTT highly depends on subjects' physical characteristics such as age, height, veining of the body. Therefore, instead of combining all measurements and generalizing PTT and BP correlation all over subjects, each subject's PTT and BP correlation is calculated separately. It is found that there are correlation between PTT1 and SBP. r is greater than 0.54 for all subjects. Calculated Person correlation coefficients of BPs and PTTs are given on Table 3, Table 4 and Table 5.

Table 3: Systolic Blood Pressure vs PTT Pearson Correlation Coefficients

<i>Systolic Blood Pressure and PTT</i>				
<i>Subjects</i>	<i>PTT1</i>	<i>PTT2</i>	<i>PTT3</i>	<i>PTT4</i>
	<i>r</i>	<i>r</i>	<i>r</i>	<i>r</i>
1	-0.69	-0.75	-0.79	-0.64
2	-0.91	-0.89	0.72	-0.45
3	-0.54	-0.81	-0.95	0.68
4	-0.94	-1.00	-0.41	-0.21
5	-0.59	-0.68	-0.52	0.56
6	-0.68	-0.44	0.98	0.72
7	-0.63	-0.60	0.18	-0.06

8	-0.79	-0.91	-0.55	-0.09
9	-0.74	-0.42	0.15	0.70
10	-0.88	-0.77	-0.24	0.64

Table 4: Diastolic Blood Pressure vs PTT Pearson Correlation Coefficients

<i>Diastolic Blood Pressure and PTT</i>				
<i>Subjects</i>	<i>PTT1</i>	<i>PTT2</i>	<i>PTT3</i>	<i>PTT4</i>
	<i>r</i>	<i>r</i>	<i>r</i>	<i>r</i>
1	-0.18	0.11	0.06	-0.99
2	-0.29	-0.06	0.77	-0.20
3	0.01	-0.28	-0.51	-0.12
4	-0.92	-0.99	-0.56	-0.37
5	0.62	0.65	0.28	-0.87
6	-0.61	-0.44	0.58	0.09
7	0.82	0.89	-0.36	0.34
8	-0.80	-1.00	-0.67	-0.44
9	-0.62	-0.80	0.44	0.27
10	-0.98	-0.99	0.10	0.83

Table 5: Mean Blood Pressure vs PTT Pearson Correlation Coefficient

<i>Mean Blood Pressure and PTT</i>				
<i>Subjects</i>	<i>PTT1</i>	<i>PTT2</i>	<i>PTT3</i>	<i>PTT4</i>
	<i>r</i>	<i>r</i>	<i>r</i>	<i>r</i>
1	-0.52	-0.41	-0.46	-0.91
2	-0.79	-0.64	0.95	-0.42
3	-0.32	-0.62	-0.83	0.35
4	-0.93	-1.00	-0.48	-0.28
5	0.03	-0.01	-0.20	-0.27
6	-0.72	-0.50	0.80	0.33
7	0.47	0.57	-0.27	0.33
8	-0.81	-0.97	-0.62	-0.25
9	-0.70	-0.63	0.31	0.50
10	-0.95	-0.89	-0.11	0.74

After the results has been reviewed, it is decided to investigate correlation by getting more experimental data from some of the subjects to increase significance of the correlation. Two of the subjects are selected whose characteristics are similar (Subject-4 and Subject-10) and have better results for further data collection. Sixteen more data recording sessions are held as eight rest and eight exercise. In addition, another vector (PTTx) is defined by combining PTT1 and PTT2 to investigate whether combined PTT would help increase the correlation. PTTx is calculated by using Equation 3. Finally, Pearson's and Spearman's correlation coefficient of PTT and BP measurements are calculated based on 20 data recording sessions for each subject. They can be found on *Table 6*, *Table 7*, *Table 8* and *Table 9*.

$$PTTx = \frac{PTT1 + PTT2}{2} \quad (4)$$

Table 6: Additional Blood Pressure and PTT measurements for subject 4 and 10

Subjects		Sessions							
		<i>Rest</i> <i>03</i>	<i>Exercise</i> <i>03</i>	<i>Rest</i> <i>04</i>	<i>Exercise</i> <i>04</i>	<i>Rest</i> <i>05</i>	<i>Exercise</i> <i>05</i>	<i>Rest</i> <i>06</i>	<i>Exercise</i> <i>06</i>
4	SBP (mmHg)	109.00	128.00	115.00	135.00	113.00	130.50	116.00	146.00
	DBP (mmHg)	71.00	80.50	75.00	82.00	72.00	78.50	70.00	84.00
	MAP (mmHg)	83.67	96.33	88.33	99.67	85.67	95.83	85.33	104.67
	PTT1 (msec)	115.00	105.00	115.00	104.00	123.00	95.00	104.00	91.00
	PTT2 (msec)	88.00	76.00	86.00	76.00	92.00	71.00	82.00	65.00
	PTT3 (msec)	253.00	113.00	173.00	279.00	100.00	185.00	217.00	40.00
	PTT4 (msec)	155.00	66.00	132.00	216.00	66.00	118.00	102.00	226.00
	PTT5 (msec)	101.50	90.50	100.50	90.00	107.50	83.00	93.00	78.00
10	SBP (mmHg)	126.00	134.50	121.00	135.50	122.00	131.50	132.00	139.00
	DBP (mmHg)	81.00	85.00	86.00	81.50	73.00	85.50	81.50	86.50
	MAP (mmHg)	96.00	101.50	97.67	99.50	89.33	100.83	98.33	104.00

	PTT1 (msec)	108.00	103.00	109.00	96.00	110.00	98.00	117.00	110.00
	PTT2 (msec)	81.00	77.00	82.00	71.00	80.00	72.00	74.00	72.00
	PTT3 (msec)	169.00	83.00	162.00	125.00	282.00	180.00	133.00	71.00
	PTT4 (msec)	41.00	16.00	7.00	92.00	140.00	140.00	399.00	10.00
	PTT5 (msec)	94.50	90.00	95.50	83.50	95.00	85.00	95.50	91.00
<hr/>									
Subjects		<i>Rest</i> 07	<i>Exercise</i> 07	<i>Rest</i> 08	<i>Exercise</i> 08	<i>Rest</i> 09	<i>Exercise</i> 09	<i>Rest</i> 10	<i>Exercise</i> 10
4	SBP (mmHg)	108.00	137.00	124.00	133.00	116.00	139.00	128.00	145.00
	DBP (mmHg)	66.00	70.00	71.00	73.00	72.00	70.00	80.00	78.50
	MAP (mmHg)	80.00	92.33	88.67	93.00	86.67	93.00	96.00	100.67
	PTT1 (msec)	111.00	88.00	111.00	89.00	111.00	88.00	106.00	80.00
	PTT2 (msec)	85.00	66.00	80.00	60.00	80.00	60.00	79.00	64.00
	PTT3 (msec)	374.00	82.00	163.00	220.00	136.00	86.00	305.00	46.00
	PTT4 (msec)	220.00	290.00	30.00	181.00	18.00	271.00	254.00	250.00
	PTT5 (msec)	98.00	77.00	95.50	74.50	95.50	74.00	92.50	72.00
10	SBP (mmHg)	130.00	133.00	138.00	146.00	136.00	142.00	134.00	130.00
	DBP (mmHg)	80.00	85.50	77.00	82.00	86.00	78.00	83.00	82.00
	MAP (mmHg)	96.67	101.33	97.33	103.33	102.67	99.33	100.00	98.00
	PTT1 (msec)	119.00	88.00	118.00	106.00	120.00	108.00	119.00	113.00
	PTT2 (msec)	72.00	67.00	72.00	73.00	75.00	69.00	75.00	79.00
	PTT3 (msec)	155.00	58.00	139.00	136.00	335.00	253.00	153.00	23.00
	PTT4 (msec)	27.00	11.00	23.00	371.00	288.00	202.00	10.00	249.00
	PTT5 (msec)	95.50	77.50	95.00	89.50	97.50	88.50	97.00	96.00

Table 7: Systolic Blood Pressure vs PTT Pearson Correlation Coefficients

Subjects	Correlation	Systolic Blood Pressure and PTT									
		PTT1		PTT2		PTT3		PTT4		PTTx	
		<i>r</i>	<i>p</i>	<i>r</i>	<i>p</i>	<i>r</i>	<i>p</i>	<i>r</i>	<i>p</i>	<i>r</i>	<i>p</i>
10	Pearson	-0.21	0.37	-0.68	0.00	-0.15	0.53	0.20	0.39	-0.42	0.07
	Spearman	-0.21	0.37	-0.65	0.00	-0.20	0.53	0.18	0.39	-0.39	0.07
4	Pearson	-0.87	0.00	-0.90	0.00	-0.52	0.02	0.42	0.07	-0.89	0.00
	Spearman	-0.86	0.00	-0.93	0.00	-0.47	0.02	0.43	0.07	-0.92	0.00

Table 8: Diastolic Blood Pressure vs PTT Pearson Correlation Coefficients

Subjects	Correlation	Diastolic Blood Pressure and PTT									
		PTT1		PTT2		PTT3		PTT4		PTTx	
		<i>r</i>	<i>p</i>	<i>r</i>	<i>p</i>	<i>r</i>	<i>p</i>	<i>r</i>	<i>p</i>	<i>r</i>	<i>p</i>
10	Pearson	-0.39	0.09	-0.29	0.21	-0.27	0.25	-0.09	0.71	-0.41	0.07
	Spearman	-0.30	0.09	-0.18	0.21	-0.19	0.25	-0.18	0.71	-0.19	0.07
4	Pearson	-0.33	0.16	-0.34	0.14	-0.19	0.43	0.12	0.62	-0.34	0.14
	Spearman	-0.23	0.16	-0.35	0.14	-0.09	0.43	0.01	0.62	-0.33	0.14

Table 9: Mean Blood Pressure vs PTT Pearson Correlation Coefficients

Subjects	Correlation	Mean Blood Pressure and PTT									
		PTT1		PTT2		PTT3		PTT4		PTTx	
		<i>r</i>	<i>p</i>	<i>r</i>	<i>p</i>	<i>r</i>	<i>p</i>	<i>r</i>	<i>p</i>	<i>r</i>	<i>p</i>
10	Pearson	-0.37	0.11	-0.60	0.00	-0.26	0.27	0.07	0.76	-0.51	0.02
	Spearman	-0.38	0.11	-0.52	0.00	-0.28	0.27	0.03	0.76	-0.41	0.02
4	Pearson	-0.68	0.00	-0.71	0.00	-0.40	0.08	0.31	0.19	-0.70	0.00
	Spearman	-0.66	0.00	-0.77	0.00	-0.31	0.08	0.30	0.19	-0.76	0.00

Correlation findings in the field of clinical research are considered as significant if $p \leq 0.05$ [40]. It has been found again that PTT2 are correlated with SBP having $r > 0.6$. The correlation coefficient is considered as strong only if its absolute value is higher than 0.6 [41]. PTT2 performs better than PTT1 and could be said to have strong correlation for both subjects ($r > 0.6, p \leq 0.01$). For Subject-4, PTT3 correlated with BP. However, for Subject-10 there is no significant correlation. PTT4 doesn't have any correlation for any of the subjects. PTTx didn't performed better than PTT2. Eventually, it can be inferred that PTT2 could be used for Blood Pressure Trending Estimation by having significant inverse linear and monotonic relationship for two blood pressures types (SBP and MBP). The graphs in Figure 5.2 and Figure 5.3 show

all data points of the experimental data collection from the two subjects and the linear line of best fit for the data combined.

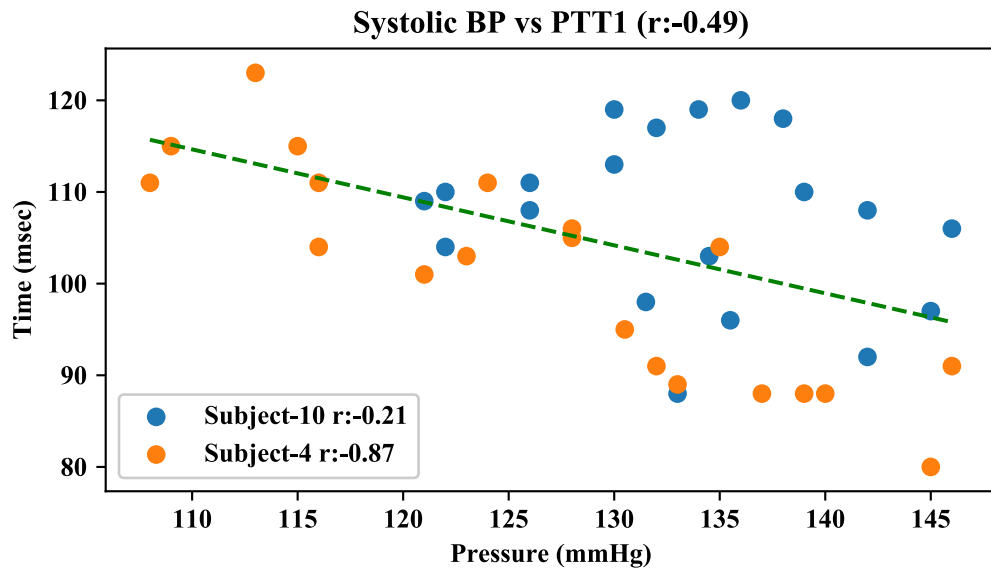


Figure 5.2: Experimental Data Points of Subject 4 and 10 for 20 session

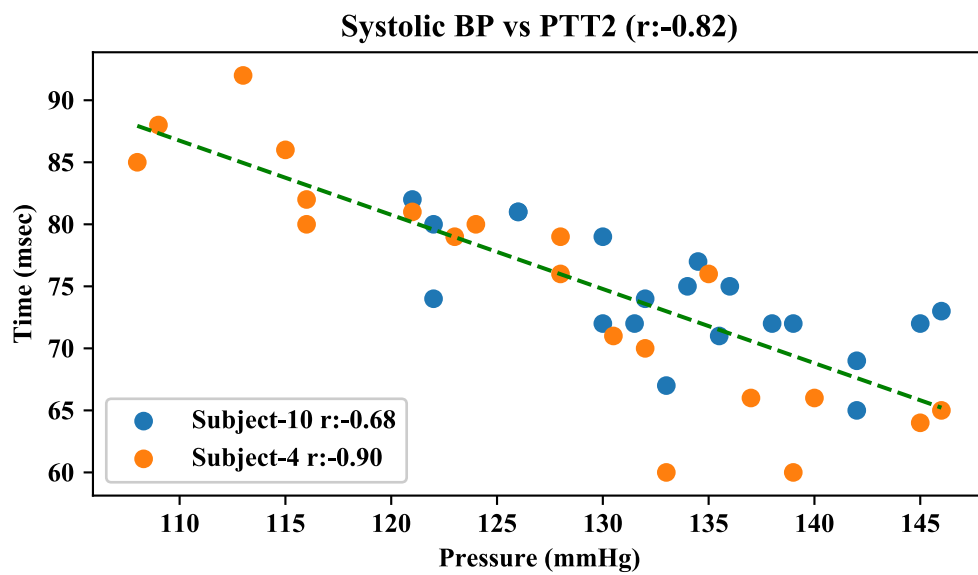


Figure 5.3: Experimental Data Points of Subject 4 and 10 for 20 session

CHAPTER 6

CONCLUSION

6.1. Discussion

The results of the study matches with the previous studies' results. It is founded many times that contact PTT (PTT1,PTT2) and SBP are negatively correlated. [9].

It is also reported that remote PTTs (PTT3, PTT4) positively and negatively correlated with SBP depend on the subject. That also matches with the results of the study in this thesis. [21]

The signal quality of the Video PPG is too low and it highly depends on environmental noises. Using IR camera and IR illumination could solve most of the noise related problems. For now, it can be though that Video PPG is unnecessary based on the results of the study, but as the image processing techniques improved the signal quality of the Video PPG is going to increase. More advanced image processing algorithms and specially designed IR camera system may contribute to remote PTT measurement and increase PTT3, PTT4 and BP correlation.

The study in this thesis is the first known study in-sync ECG&PPG IC sensor is used [26]. It has been proven that sensors like MAX86150 could be used to measure PTT without the need for synchronization. Simple design modifications could enable PTT measurements from smartphones and smartwatches thanks to the new IC.

Some of the smartphones are already equipped with PPG sensor, replacing the sensor with the new one doesn't require any major change. ECG pads can be connected to antennas of the phones which are located at right and left edge of the smartphones. Holding the phone as described in *Figure 1.4* allow PTT measurements comfortably.

Some smartwatches are already equipped with both ECG and PPG. Manufacturers could enable contact PTT measurement only by using the IC as single sensor.

The biggest challenge in this study was gathering experimental data from volunteer subjects. To date, the most participatory study (having rPTT measurement) on this topic has 29 volunteers [21]. The design changes described could allow the more data collected from the more user. If there will be a study open to public like Apple Heart study, better results can be obtained. Rather than simple linear regression, more advanced algorithms could be developed based on the amount of data collected.

It is observed that for an healthy adult, the body tolerates the blood pressure change created by exercise very quickly. Therefore, it should also be noted that changing blood pressure levels by having exercises may not be the best way. Rather than getting experimental data right after instant blood pressure changes, getting the data when blood pressure is stabilized may lead better results. That again emphasizes the importance of a mobile data collection device which can be used anytime, anywhere.

6.2. Conclusion

In this thesis, it is hypothesized that blood pressure trending (increased or decreased state of SBP compare to its previous state) can be estimated with smartphones by utilizing the components that are available today.

To validate the hypothesis, a method for blood pressure trending estimation has been proposed and tested. The proposed method is mainly based on different kinds of PTT measurements and their correlation with BP. To test the method, an experimental system that can be packed into a smartphone has been designed. The designed system consists of a High-Speed Camera and ECG&PPG IC sensor. A data collection setup and procedure are established based on the designed system to collect experimental data.

During experimental data collection sessions, single lead ECG, fingertip PPG, and vPPG measurements are taken from ten volunteer subjects. Combining ECG and PPG

waveforms, four different PTT measurements are calculated for each subject. Then, correlation of PTTs and BP are evaluated based on the Person's and Spearman's Correlation Coefficients.

Initially, it was thought that an increasing number of different kinds of PTT measurements would increase the accuracy of BP trending estimation. However, only PTT2 performed well. Results of the study showed that there is negative linear correlation between PTT2 (time delay between ECG-R wave and fingertip PPG waveform's peak) and Systolic Blood Pressure. Magnitude of " r "s for each correlation test (Pearson's and Spearman's) are greater than 0.6 and " p " are lower than 0.01 for PTT2 and BP which indicates results are statistically reliable [40], [41]. For the other PTT measurements, there is a strong correlation with BP for some of the subjects. However, it is not generalizable. While for some subjects, correlation is negative; for others, it is positive. Therefore, there should be more research to be done on this topic to find new methods to increase correlation.

In conclusion, the study in this thesis showed that as measured SBP increases PTT2 decreases and vice versa for all subjects. The correlation coefficient in this study is not the best among the studies in the literature, but it supports the claim of BP and PTT2 are negatively correlated. By comparing PTT2 values taken at different time instances, blood pressure trends can be estimated. If measured PTT2 is lowered, BP is expected to be increased and vice versa. Hence, this relationship paves the way to estimate trend of SBP with smartphones. The smartphones equipped with MAX86150 could tell their users that their SBP is increased/decreased compared to the average, utilizing the negative linear correlation in the near future. If a feature like this is made public to users, it will make the data to be collected from millions of people possible. Having collected data from millions of people can eventually enable SBP and DBP measurement, not just trending with a smartphone by developing advanced algorithms rather than simple linear regression. It should be noted that more research should be done and more data should be collected to produce a medical grade product.

6.3. Future Work

The following improvements should be done in the future studies;

- Increasing PPG&ECG IC sensor's and video camera's sample rate to 1600Hz
- Obtaining more experimental data from more subjects
- Designing and producing a conceptual smartphone or smartphone case that makes data collection easier than ever.
- Applying more advanced regression algorithms to the data collected to get better cuff less BP trending estimation or measurement.

REFERENCES

- [1] C. M. Lawes, S. Vander Hoorn, and A. Rodgers, “Global burden of blood-pressure-related disease, 2001,” *Lancet*, 2008.
- [2] G. Ogedegbe and T. Pickering, *Principles and Techniques of Blood Pressure Measurement*. 2010.
- [3] S. V. Ákos Jobbágy, *Biomedical Instrumentation*. Typotex Kiadó, 2014.
- [4] H. Sorvoja and R. Myllylä, “Noninvasive Blood Pressure Measurement Methods,” *Mol. Quantum Acoust.*, vol. 27, pp. 239–264, 2006.
- [5] J. A. Topouchian, M. A. El Assaad, L. V Orobinskaia, R. N. El Feghali, and R. G. Asmar, “Validation of two automatic devices for self-measurement of blood pressure according to the International Protocol of the European Society of Hypertension: the Omron M6 (HEM-7001-E) and the Omron R7 (HEM 637-IT),” *Blood Press. Monit.*, vol. 11, no. 3, pp. 165–71, Jun. 2006.
- [6] L. A. Geddes, M. Voelz, S. James, and D. Reiner, “Pulse wave velocity as a method of obtaining systolic and diastolic blood pressure,” *Med. Biol. Eng. Comput.*, vol. 19, pp. 671–672, 1982.
- [7] M. Okada, “Possible Determinants of Pulse-Wave Velocity in Vivo,” *IEEE Trans. Biomed. Eng.*, vol. 35, no. 5, pp. 357–361, 1988.
- [8] D. Franchi *et al.*, “Blood pressure evaluation based on arterial pulse wave velocity,” 1996, pp. 397–400.
- [9] A. Patzak, Y. Mendoza, H. Gesche, and M. Konermann, “Continuous blood pressure measurement using the pulse transit time: Comparison to intra-arterial measurement,” *Blood Press.*, vol. 24, no. 4, pp. 217–21, 2015.
- [10] E. F. Grenaker, “Radar sensing of heartbeat and respiration at a distance with

- applications of the technology,” in *Radar Systems (RADAR 97)*, 1997, vol. 1997, pp. 150–154.
- [11] M. Garbey, N. Sun, A. Merla, and I. Pavlidis, “Contact-free measurement of cardiac pulse based on the analysis of thermal imagery,” *IEEE Trans. Biomed. Eng.*, vol. 54, no. 8, pp. 1418–1426, Aug. 2007.
 - [12] M.-Z. Poh, D. J. McDuff, and R. W. Picard, “Non-contact, automated cardiac pulse measurements using video imaging and blind source separation,” *Opt. Express*, vol. 18, no. 10, p. 10762, May 2010.
 - [13] M. Lewandowska, J. Rumiński, T. Kocejko, and J. Nowak, “Measuring pulse rate with a webcam - A non-contact method for evaluating cardiac activity,” in *2011 Federated Conference on Computer Science and Information Systems, FedCSIS 2011*, 2011, pp. 405–410.
 - [14] G. De Haan and V. Jeanne, “Robust pulse rate from chrominance-based rPPG,” *IEEE Trans. Biomed. Eng.*, vol. 60, no. 10, pp. 2878–2886, 2013.
 - [15] L. Iozzia, L. Cerina, and L. T. Mainardi, “Assessment of beat-to-beat heart rate detection method using a camera as contactless sensor,” *Proc. Annu. Int. Conf. IEEE Eng. Med. Biol. Soc. EMBS*, vol. 2016-Octob, pp. 521–524, 2016.
 - [16] F. Schruppf, J. Bauer, B. Reichard, D. Matthes, and M. Fuchs, “Camera-based pulse transition time measurement for blood pressure estimation,” no. September, 2016.
 - [17] M. Van Gastel, S. Stuijk, and G. De Haan, “Motion robust remote-PPG in infrared,” *IEEE Trans. Biomed. Eng.*, vol. 62, no. 5, pp. 1425–1433, May 2015.
 - [18] A. Lindqvist and M. Lindelöw, “Remote Heart Rate Extraction from Near Infrared Videos.”
 - [19] W. Chen, J. Hernandez, and R. W. Picard, “Estimating carotid pulse and breathing rate from near-infrared video of the neck,” *Physiol. Meas.*, vol. 39,

no. 10, Oct. 2018.

- [20] I. C. Jeong and J. Finkelstein, “Introducing Contactless Blood Pressure Assessment Using a High Speed Video Camera,” *J. Med. Syst.*, vol. 40, no. 4, pp. 1–10, 2016.
- [21] G. Zhang, C. Shan, I. Kirenko, X. Long, and R. M. Aarts, “Hybrid optical unobtrusive blood pressure measurements,” *Sensors (Switzerland)*, vol. 17, no. 7, Jul. 2017.
- [22] “Sensor Extension | SAMSUNG Developers.” [Online]. Available: <https://developer.samsung.com/galaxy/sensor-extension>. [Accessed: 02-Dec-2019].
- [23] N. Paradkar and S. R. Chowdhury, “Cardiac arrhythmia detection using photoplethysmography,” *Conf. Proc. ... Annu. Int. Conf. IEEE Eng. Med. Biol. Soc. IEEE Eng. Med. Biol. Soc. Annu. Conf.*, vol. 2017, pp. 113–116, 2017.
- [24] Apple Inc., “Using Apple Watch for Arrhythmia Detection,” 2018.
- [25] Malcolm Owen, “ECG feature in Apple Watch is already saving lives,” 2018. [Online]. Available: <https://appleinsider.com/articles/18/12/07/ecg-feature-in-apple-watch-is-already-saving-lives>. [Accessed: 17-Aug-2019].
- [26] L. Dolan, “Maxim’s Integrated PPG and ECG Biosensor Module for Mobile is an Industry First,” 2019. .
- [27] “Why the Apple iPhone X matters to smart homes | SIMON LAKEY.” [Online]. Available: <https://simonlakey.com/why-the-apple-iphonex-matters/>. [Accessed: 02-Dec-2019].
- [28] E. N. Marieb, *Essentials of human anatomy and physiology*. Benjamin Cummings, 2003.
- [29] H. V. Sparks and T. W. Rooke, *Essentials of Cardiovascular Physiology*. University of Minnesota Press, 1987.

- [30] E. A. Ashley and J. Niebauer, “Conquering the ECG,” 2004.
- [31] Y. Xu, P. Ping, D. Wang, and W. Zhang, “Analysis for the Influence of ABR Sensitivity on PTT-Based Cuff-Less Blood Pressure Estimation before and after Exercise,” *J. Healthc. Eng.*, vol. 2018, p. 5396030, 2018.
- [32] Z. Taha, L. Shirley, and M. A. Mohd Razman, “A review on non-invasive hypertension monitoring system by using photoplethysmography method,” *Movement, Heal. Exerc.*, vol. 6, no. 1, 2017.
- [33] “MAX86150 Integrated Photoplethysmogram and Electrocardiogram Bio-Sensor Module For Mobile Health - Maxim.” [Online]. Available: <https://www.maximintegrated.com/en/products/sensors/MAX86150.html>. [Accessed: 02-Dec-2019].
- [34] “MAX86150 Evaluation Kit (MAX86150EVSYS#) - Maxim | Mouser Turkey.” [Online]. Available: <https://www.mouser.com.tr/new/maxim-integrated/maxim-max86150-eval-kit/>. [Accessed: 02-Dec-2019].
- [35] P. Viola and M. Jones, “Rapid object detection using a boosted cascade of simple features,” pp. I-511-I-518, 2005.
- [36] “dlib C++ Library.” [Online]. Available: <http://dlib.net/>. [Accessed: 02-Dec-2019].
- [37] G. Balakrishnan, F. Durand, and J. Guttag, “Detecting pulse from head motions in video,” in *Proceedings of the IEEE Computer Society Conference on Computer Vision and Pattern Recognition*, 2013, pp. 3430–3437.
- [38] L. Zheng, C. Lall, and Y. Chen, “Low-distortion baseline removal algorithm for electrocardiogram signals,” *Comput. Cardiol. (2010).*, vol. 39, pp. 769–772, 2012.
- [39] D. DeMers and D. Wachs, *Physiology, Mean Arterial Pressure*. 2019.
- [40] J. F. Box, *R.A. Fisher, the life of a scientist*. Wiley, 1978.

- [41] H. Akoglu, “User’s guide to correlation coefficients,” *Turkish Journal of Emergency Medicine*, vol. 18, no. 3. Emergency Medicine Association of Turkey, pp. 91–93, 01-Sep-2018.

APPENDICES

A. Consent Form

ARAŞTIRMAYA GÖNÜLLÜ KATILIM FORMU

Bu araştırma, ODTÜ Elektrik ve Elektronik Mühendisliği Bölümü yüksek lisans öğrencisi Atıf Emre Ofloğlu tarafından yürütülen bir çalışmadır. Bu form sizi araştırma koşulları hakkında bilgilendirmek için hazırlanmıştır.

Çalışmanın Amacı Nedir? Araştırmmanın amacı “EKG ve PPG sinyalleri kullanarak tansiyon trendini tahmin etmek” tir. Araştırmaya katılmayı kabul ederseniz, sizden beklenen, kendinizi iyi hissettiğiniz bir günde sizin için özel hazırlanmış kamera, EKG&PPG sensör ve tansiyon aleti içeren veri toplama sistemi içeren bir veya birden çok veri toplama seansında yer almanız ve veri toplama prosedürüne uymanızdır. Bu çalışmaya katılım her bir seans için ortalama olarak 30 dakika sürmektedir.

Bize Nasıl Yardımcı Olmanızı İsteyeceğiz? Sizden bir sandalyeye oturmanız, size doğru bakan ve sadece yüzünüzü kayda alacak şekilde ayarlanmış bir kameraya bakmanız ve aynı zamanda sağ işaret parmağınızı PPG sensörünün üzerine koymanız istenecektir. Buna ek olarak sağ ve sol bileklerinize ve sol avuç içinize EKG elektrotları yapıştırılacaktır. Bu sayede sizden yüzünüzün video kaydı, parmak PPG ve EKG sinyalleriniz toplanacaktır. Her veri toplama seansı 4 kısımdan oluşmaktadır. Bu kısımlar arasında gönüllülerin tansiyon değerlerinin değiştirilmesi hedeflenmektedir. Bu yüzden her bir seans için 2 kez olmak üzere gönüllülerden 1 ve 2 dakika sürecek basit egzersizler yapmaları, bu sayede tansiyon değerlerini yükseltmeleri istenecektir. Egzersizler kısa süreli koşu, zıplama, şınav ve mekikten oluşmaktadır.

Her gönüllüden kendi istediği egzersizi seçmesi istenecektir ve kendini yorgun hissettiği ana veya egzersiz süresi dolana egzersizi yapması istenecektir.

Sizden Topladığımız Bilgileri Nasıl Kullanacağız? Araştırmaya katılımınız tamamen gönüllülük temelinde olmalıdır. Çalışma süresince, sizden kimlik veya kurum belirleyici hiçbir bilgi istenmemektedir. Kişisel bilgileriniz tamamıyla anonim tutulacak, sadece araştırmacılar tarafından değerlendirilecektir. Katılımcılardan elde edilecek bilgiler toplu halde değerlendirilecek ve bilimsel yayımlarda kullanılacaktır. Sağladığınız veriler gönüllü katılım formlarında toplanan kimlik bilgileri ile eşleştirilmeyecektir.

Katılımınızla ilgili bilmeniz gerekenler: Çalışmaya katılım sağlarken veri toplama seansları sırasında herhangi başka bir nedenden ötürü kendinizi rahatsız hissederseniz seansı yarıda bırakıp çıkmakta serbestsiniz. Böyle bir durumda çalışmayı uygulayan kişiye, seansı sonlandırmak istediğinizi söylemek yeterli olacaktır. Çalışma sonunda, bu araştırmayla ilgili sorularınız cevaplanacaktır.

Araştırmayla ilgili daha fazla bilgi almak isterseniz: Bu çalışmaya katıldığınız için şimdiden teşekkür ederiz. Araştırma hakkında daha fazla bilgi almak için ODTÜ Elektrik ve Elektronik Mühendisliği Bölümü yüksek lisans öğrencisi Atıf Emre Ofluoğlu (E-posta: emre.ofluoglu@metu.edu.tr) ile iletişim kurabilirsiniz.

Yukarıdaki bilgileri okudum ve bu çalışmaya tamamen gönüllü olarak katılıyorum.

(Formu doldurup imzaladıktan sonra uygulayıcıya geri veriniz).

İsim Soyad

Tarih

İmza

---/---/---